Design, Synthesis, and Evaluation of Fluorinated Radioligands for Myelin Imaging

Anand Dev Tiwari,[†,#] Chunying Wu,[†,#] Junqing Zhu,[†] Sheng Zhang,[†] Jinle Zhu,[†,○] William R. Wang,[†,∇] Jinming Zhang,[‡] Curtis Tatsuoka,[§] Paul M. Matthews,[∥] Robert H. Miller,[⊥] and Yanming Wang*,[†]

[†]Department of Radiology and [§]Department of Epidemiology and Biostatistics, Case Western Reserve University, Cleveland, Ohio 44106, United States

[‡]Department of Nuclear Medicine, People's Liberation Army (PLA) General Hospital, Beijing 100853, China

[∥]Division of Brain Sciences, Department of Medicine, Imperial College London, London SW12 0NN, United Kingdom

[⊥]Department of Anatomy and Regenerative Biology, George Washington University, Washington, DC 20037, United States

Ⓢ *Supporting Information*
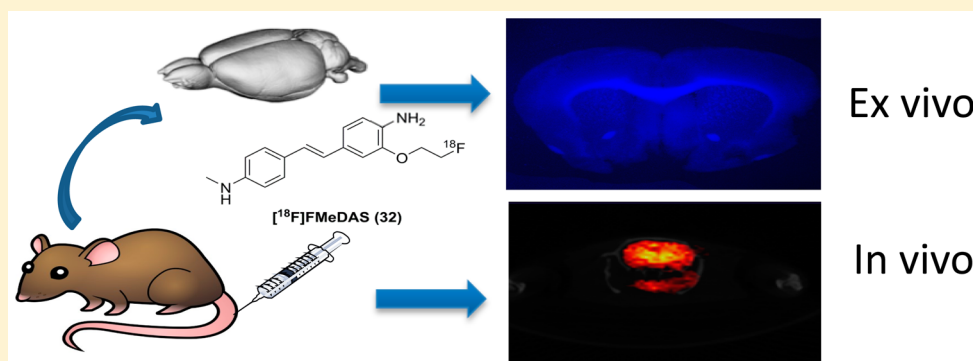
ABSTRACT: Myelination is one of the fundamental processes in vertebrates. A major challenge is to quantitatively image myelin distribution in the central nervous system. For this reason, we designed and synthesized a series of fluorinated radioligands that can be radiolabeled as radiotracers for positron emission tomography (PET) imaging of myelin. These newly developed radioligands readily penetrate the blood−brain barrier and selectively bind to myelin membranes in the white matter region. Structure−activity relationship studies of such ligands suggested that optimal permeability could be achieved with calculated lipophilicty in the range of 3−4. After radiolabeling with fluorine-18, the brain uptake and retention of each radioligand were determined by microPET/CT imaging studies. These pharmacokinetic studies led us to identify a lead compound ([¹⁸F]FMeDAS, **32**) with promising in vivo binding properties, which was subsequently validated by ex vivo autoradiography.

■ INTRODUCTION

Myelination is one of the fundamental biological processes in the vertebrate nervous system that involves formation of layers of dielectric myelin sheaths around axons.[1] Myelin sheaths help insulate axons from electrically charged media present in the nervous system to allow efficient signal transduction. It is critical to maintain the integrity of myelin throughout the nervous system so that action potentials can be propagated along myelinated axons over long distances and at high rates. However, there are numerous medical conditions where myelin sheaths are irreversibly damaged thus causing neurological disorders such as multiple sclerosis (MS) and leukodystrophies in the central nervous system and neuropathies in the peripheral nervous system.[2,3]

Currently, conventional magnetic resonance imaging (MRI), such as T1 or T2-weighted MRI, has been widely used as a primary imaging modality to detect lesions formed in the brain and spinal cord.[4] However, lesions detected by MRI only reflect

a change in tissue water content, which is a nonspecific measure of the overall changes in macroscopic tissue injury that ranges from edema inflammation to demyelination and axonal loss.[5] As a result, the use of MRI as a primary outcome measure of disease activity has been shown to be unassociated with clinical outcomes,[6] which makes it difficult for accurate diagnosis and prognosis. To overcome this clinico-radiological paradox, several MRI techniques such as diffusion tensor imaging (DTI) and magnetization transfer ratio (MTR), and gadolinium-DTPA enhancement have been used in order to improve the correlation of lesion loads with disease activities. However, these new techniques still do not provide sensitive and quantitative measures with robust reproductively across different facilities.[7−9]

This long-standing clinico-radiological paradox exists due to the fact that MS and related neurological disorders are characterized by demyelination, while MRI signals only reflect a change in tissue water content. To address this challenge, we originally proposed to use positron emission tomography (PET), which is a widely used clinical imaging modality with high sensitivity and quantitation capability.[10] When used in combination with radiotracers that are specific for myelin, PET is capable to detect and quantify myelin changes in the central nervous system (CNS).[11−13] In 2006 we set out to develop myelin-targeted molecular probes that readily enter the brain and bind to myelin with high affinity and specificity.[14] Since then, we have developed a wide array of myelin-specific probes based on different pharmacophores.[15,16] When labeled with positron-emitting C-11, some of the selected agents have been successfully used as radiotracers for PET imaging of myelination in various animal models in a longitudinal fashion.[16−19]

We have demonstrated proof-of-principle for using PET as an imaging end point for disease stratification and monitoring treatment response for myelin therapies with [N-methyl-^{11}C]-4,4′-diaminostilbene [^{11}C]MeDAS as our lead radiotracer.[19−22] Although use of C-11 radiotracers minimizes radiation exposure to patients, the 20 min half-life of C-11 makes them impractical for remote distribution. This often limits their use in medical facilities that are without on-site cyclotron and radiochemistry facilities. This limitation can be overcome by using fluorine-18-labeled radiotracers which have a relatively long half-life of 110 min that makes regional distribution from a central radio-pharmacy feasible.[23−26] Thus, F-18-labeled analogs need to be developed. In order to enhance the potential of our previously developed C-11-labeled radiotracers for routine clinical use, we set out to develop F-18-labeled MeDAS analogs ([^{18}F]-FMeDAS) for myelin imaging.

In the present study, we report the design, synthesis, radiolabeling, and microPET imaging studies of a series of fluorinated MeDAS analogs.

■ RESULTS AND DISCUSSION

Chemistry. The design of the fluorinated radioligands is based on the structure of MeDAS, a lead myelin-specific radioligand that we previously developed for PET imaging of myelination. Structure−activity relationship studies suggested that fluorine could be introduced through alkylation of the amino groups, which are responsible for binding to myelin.[27] Once various fluorinated alkyl groups are introduced to MeDAS, the derivatives produced may have different lipophilicity and permeability across the blood−brain barrier (BBB). Thus, the newly synthesized fluorinated analogs, even though they share the same pharmacophore as MeDAS, may display distinctly different physicochemical and biological properties. Thus, we conducted a systematic evaluation of the in vitro and in vivo properties of binding to myelin.

Our previous structure−activity relationship studies suggested that the two amino groups can be modified but cannot be replaced, as they both are responsible for myelin binding.[28] Thus, we introduced fluorine to MeDAS via an aliphatic ether side chain in the beta-position to the amino group. Introduction of fluorine often reduces the lipophilicity of compounds.[27] We thus synthesized a series of fluorinated MeDAS analogs by alkylating the other amino group opposite to the fluorinated alkyl amino group.

The lipophilicity of these compounds was calculated using ALOGPS 2.1 program (Virtual Computational Chemistry Laboratory). As shown in Table 1, the calculated lipophilicity

**Table 1. Structures of a List of FMeDAS Agents Synthesized with Calculated logP Value**

Entry	Structure	clogP
MeDAS		3.39
25		2.78
32		3.65
33		4.23
34		4.68
35		4.48
36		5.27
37		2.75
39		3.65

(cLogP) of these newly synthesized compounds ranges from 2.7 to 5.4. Such a range provides a good spectrum of lipophilicity for us to navigate the in vitro and in vivo binding properties.

As shown in Scheme 1, various tosylated nitrobenzaldehydes (3, 4, 6) and fluorinated nitrobenzaldehydes (5, 7) were first prepared from 3-hydroxy-4-nitrobenzaldehyde (1) and 4-hydroxy-3-nitrobenzaldehyde (2) in 50−90% yield.[29]

For the synthesis of fluorinated MeDAS analogs except compound 25, we started with p-aminobenzyldiethyl phosphonate (8). As shown in Scheme 2, the amino group was first protected with Boc to generate compound 9 in 95% yield, which was subsequently alkylated with different alkyl iodides to obtain compounds 10−14 in 20 to 80% yield.

The Boc-protected-N-alkylated diethyl benzylphosphonate and diethyl (4-nitrobenzyl)phosphonate (10−15) were coupled with tosylated nitrobenzaldehydes (3, 4, 6) to produce the radiolabeling precursors (16−23) through the Horner−Wadsworth−Emmons reaction (Schemes 3 and 4) in 40 to 80% yield. These precursors (16−23) were used for the radiosynthesis of F-18-labeled MeDAS analogs.

Scheme 1. Synthesis of Tosylated and Fluorinated Nitrobenzaldehyde Derivative (3–7)[a]
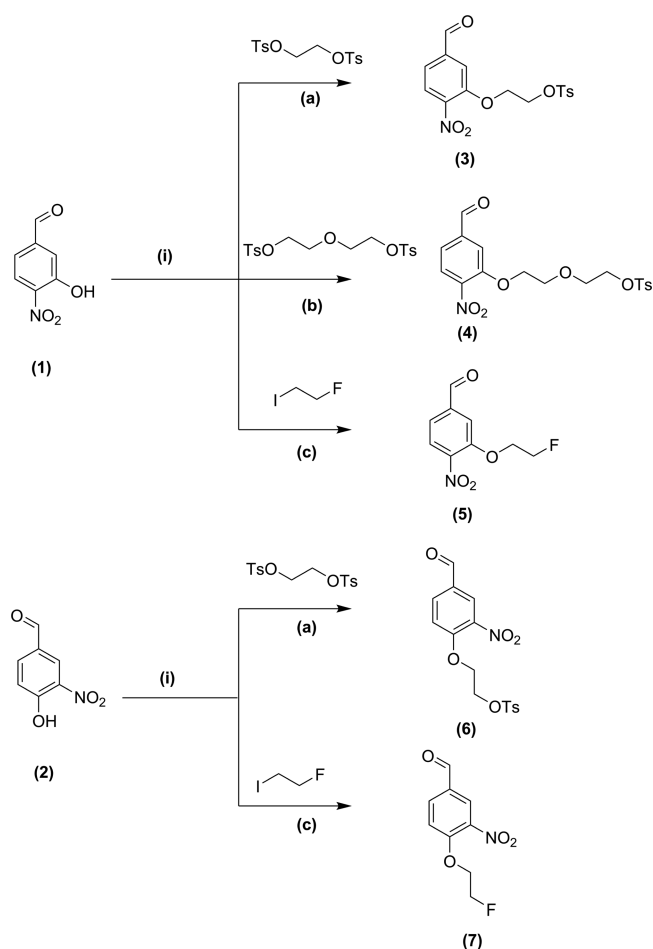
[a]Reagents and conditions: (i) K_2CO_3, DMF, 80 °C, 6 h, yield 50–90%

For the synthesis of compound **25**, the tosylated compound **23** was subjected to a nucleophilic substitution to generate compound **24** in 80% yield followed by reduction of the nitro group to give the final cold standard compound **25** in 50% yield (Scheme 4).

For the synthesis of the remainder of fluorinated compounds **32–37** and **39**, fluorinated nitrobenzaldehydes (**5**, **7**) and compounds **10–15** were coupled to produce intermediates **26–31** and **38** in 40–60% yield (Scheme 5). This was followed by a one-pot reaction using $SnCl_2$ in ethanol and ethyl acetate, which allowed for simultaneous deprotection of the Boc group

and reduction of the nitro group to the amino group of compounds **26–31** and **38** in 30–90% yield to generate final compounds **32–37** and **39** that can be used as standards for radiochemistry synthesis as well as for biological evaluations.[28,30]
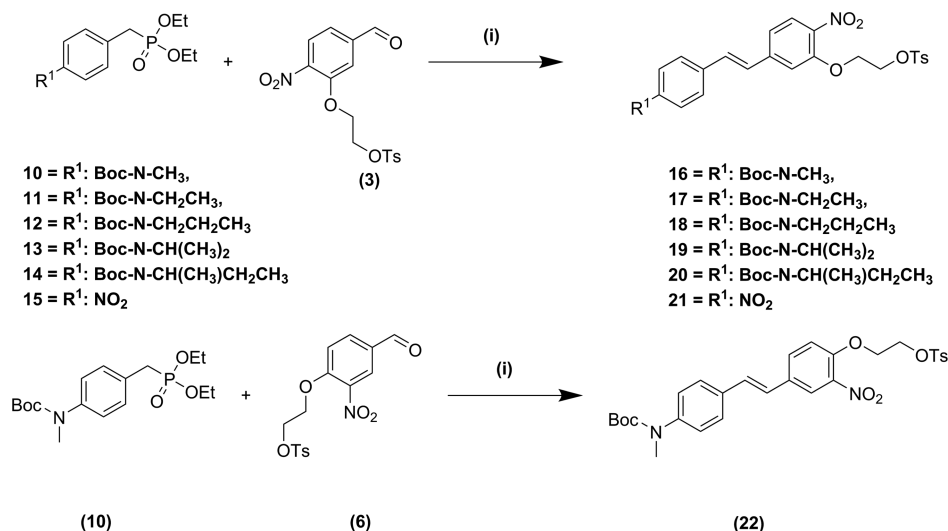
Similar to MeDAS, all of the newly synthesized fluorinated analogs are fluorescent. The excitation/emission spectra were acquired in acetonitrile for comparison as shown in Figure 1. The excitation wavelengths of these compounds were measured to be 390 ± 10 nm, and the emission wavelengths were measured to be 420 ± 10 nm. Such wavelengths are in an ideal range to conduct fluorescent tissue staining which allows examination of the preliminary binding specificity for myelin, either in vitro or in situ.

In Vitro Staining and Assay of the Fluorescent Intensity. In vitro fluorescent tissue staining provides a convenient way to screen binding specificity of the newly synthesized compounds for myelin. Myelin sheaths are distributed more dominantly in the white matter than in the gray matter. Thus, the fluorescent intensity is expected to be consistent with the pattern of myelin distribution in the brain. As expected, in vitro tissue staining of mouse brain sections showed that all target compounds (**25**, **32–37**, and **39**) selectively stained myelinated regions such as corpus callosum and striatum. In order to compare the binding feature for myelin by in vitro histological staining of mouse brain tissue sections, all compounds were tested at same time, the concentration of all the tested staining solution was 1 mM, and sections were imaged under the same exposure time after being incubated with the staining solution for 25 min. Next, we selected a representative region in the genu of the corpus callosum (gcc) and a representative region in the subcortical gray matter (cortex) and calculated the fluorescent intensity ratio (FIR) between both regions (Figure 2A). This allowed us to preliminarily compare the binding specificity for myelin. As shown in Figure 2B, the newly synthesized compounds can be divided into two groups, with two of the compounds (**32** and **35**) showing a FIR > 2 and the rest of them <2. The higher FIR indicates a higher degree of specific binding. This study suggested that compounds **32** and **35** be the lead candidates for further evaluation.

Ex Vivo Imaging. The newly synthesized fluorescent compounds are also suitable for in situ tissue staining through direct tail vein injection. This study allowed us to determine both brain permeability as well as in vivo binding specificity. Thus, ex vivo imaging was performed following in vitro tissue staining. At a dose of 40 mg/kg, each tested compound was administered to mice through tail vein injection. Use of high concentration is needed to enable fluorescence visualization ex

Scheme 2. Synthesis of Alkylated *tert*-Butyl (4-((diethoxyphosphoryl)methyl)phenyl)carbamate (10–14)[a]

10: $R^1 = CH_3$
11: $R^1 = CH_2CH_3$
12: $R^1 = CH_2CH_2CH_3$
13: $R^1 = CH(CH_3)_2$
14: $R^1 = CH(CH_3)CH_2CH_3$
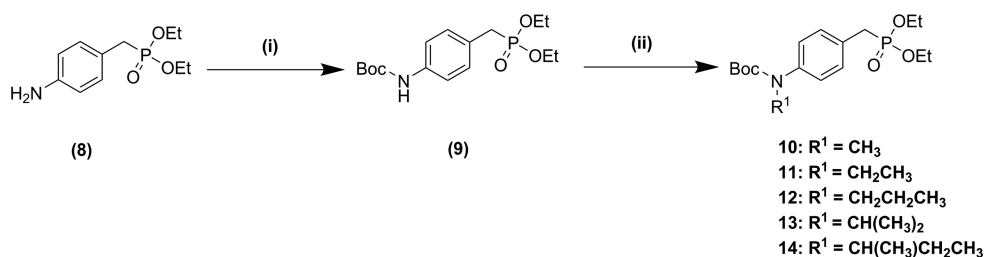
[a]Reagents and conditions: (i) (Boc)$_2$O, THF:H$_2$O (3:1), 20 °C, 48 h, yield 95%; (ii) NaH (95%), R^{1}I, anhydrous THF, 0–20 °C, 12 h, yield 75 to 20%.

Scheme 3. Synthesis of Tosylated Precursor of MeDAS Analogue for the [¹⁸F]-Labeling (16−22)[a]

10 = R¹: Boc-N-CH₃,
11 = R¹: Boc-N-CH₂CH₃,
12 = R¹: Boc-N-CH₂CH₂CH₃
13 = R¹: Boc-N-CH(CH₃)₂
14 = R¹: Boc-N-CH(CH₃)CH₂CH₃
15 = R¹: NO₂

(3)

16 = R¹: Boc-N-CH₃,
17 = R¹: Boc-N-CH₂CH₃,
18 = R¹: Boc-N-CH₂CH₂CH₃
19 = R¹: Boc-N-CH(CH₃)₂
20 = R¹: Boc-N-CH(CH₃)CH₂CH₃
21 = R¹: NO₂

(10)   (6)   (22)

[a]Reagents and conditions: (i): NaH (60%), anhydrous DMF, 0 °C, 4 h, yield 40−80%.

Scheme 4. Synthesis of Compound 25[a]

(15)   (4)   (23)
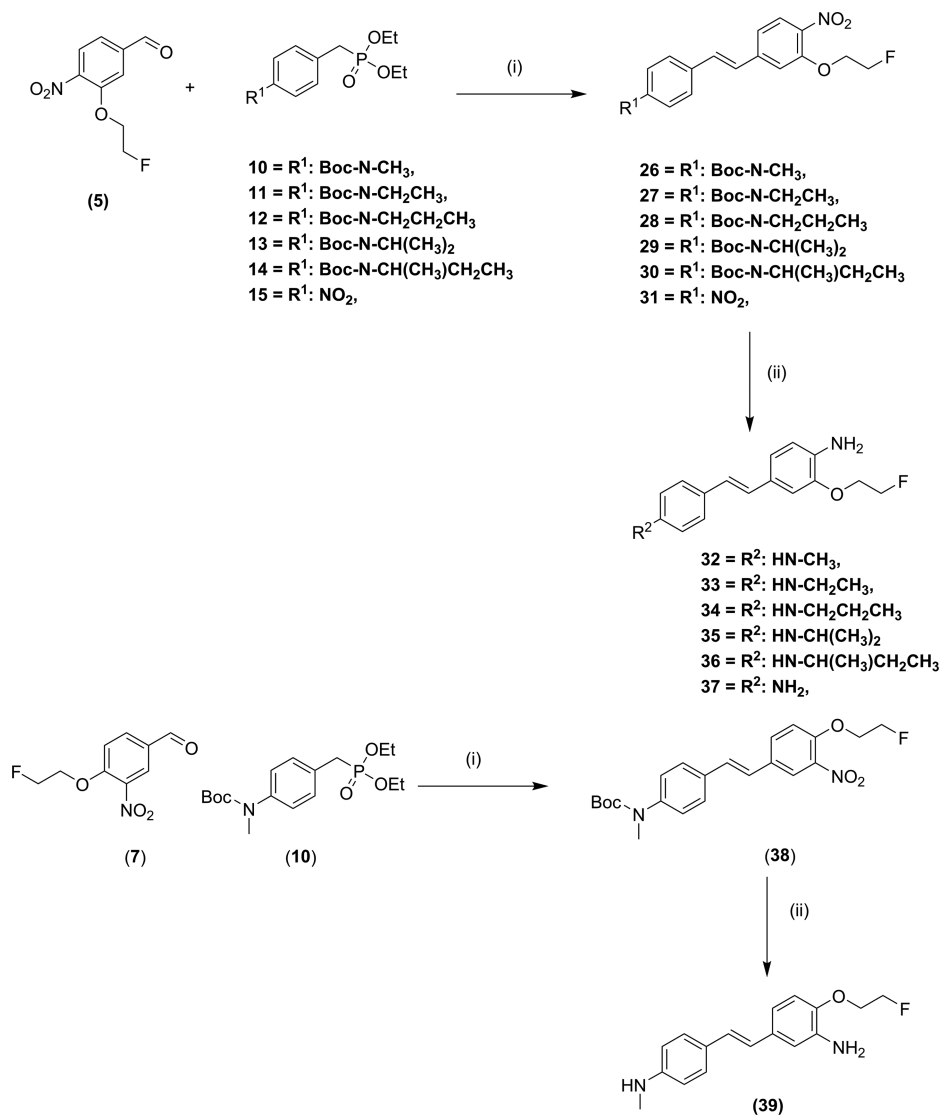
(25)   (24)
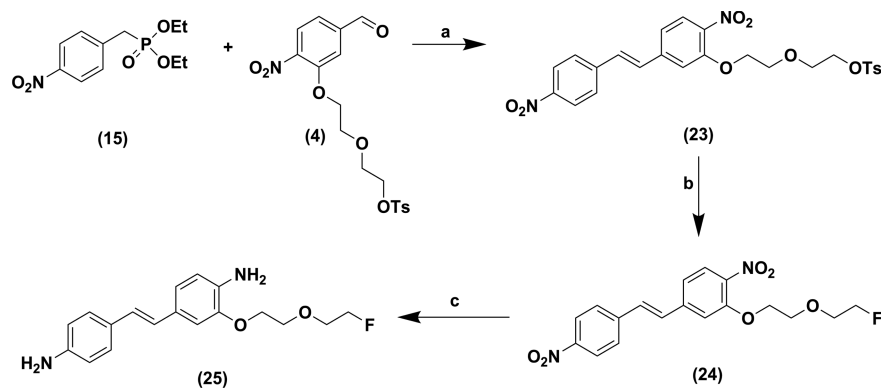
[a]Reagents and conditions: (a) NaH (60%), DMF, 0 °C, 2 h, yield 80%. (b) K_{222}, CsF, MeCN, 80 °C, 4 h, yield 84%. (c) SnCl₂, EtOAc:EtOH (3:2) 80 °C, 6 h, yield 47%.

vivo. As shown in Figure 3, the two lead compounds readily enter the brain and specifically bind to myelin tracts present in the white matter regions such as the corpus callosum and striatum. In fact, all the newly synthesized compounds can penetrate the BBB and selectively localize in the white matter region (Supporting Information Table S1). Such in situ staining, however, is only a qualitative and insensitive measure to determine brain permeability. The injected amounts are in the range of 40 mg/kg, which is at least 3 orders of magnitude greater than in vivo PET imaging.

Radiosynthesis. Encouraged by the above results, we then evaluated the in vivo pharmacokinetic profiles of the newly synthesized compounds labeled with positron emitting fluorine-18. The radiosynthesis was achieved through nucleophilic substitution of a tosylate group, as shown in Schemes 6, 7, and 8, with fluorine-18 generated by an onsite cyclotron followed by a reduction and/or acidic hydrolysis of the Boc protection group. In this study, the tosylated precursor was employed in a three-step radiosynthesis starting with a nucleophilic substitution with ¹⁸F⁻ in the presence of K₂CO₃ and Kryptofix (K₂₂₂) in MeCN at 115 °C for 10 min. After evaporation of MeCN, more than $91 \pm 7\%$ ($n = 15$) of the activity was retained in the reaction vessel. The fluorinated intermediate

was simply purified by passing through a silica Sep-Pak to remove unreacted free fluorine-18. The fluorinated intermediate (60−80%) was then reduced by SnCl₂ in hydrochloric acid and ethanol at 120 °C for 10 min to yield the primary amine (compound **25** and **37**). At this step, it was necessary to extend the reaction time if the acidic hydrolysis of the Boc protecting group is needed (compound **32−36** and **39**). After cooling to room temperature, the reactant was neutralized to pH 8−9 by addition of NaOH (1.0 M, 0.8 mL) and was further purified by semipreparative HPLC to yield the final products with modest yields (for the three-step procedure) ranging from 30−60% (decay corrected to the end of bombardment (EOB)) within 120−130 min.[31]

The identities of the products were confirmed using HPLC by co-injection with each cold standard compound. Radio-chemical purity (RCP) of final products was over 98% determined by analytical radio-HPLC. The specific activity at the end of synthesis was in a range of 0.55−2.5 Ci/μmol. All the [¹⁸F]-labeled compounds were stable after being allowed to stand at room temperature for 4 h or diluted with saline. The radiochemical purity of both the original and diluted aqueous solutions was >95% determined by analytical HPLC.

Scheme 5. Synthesis of Fluorinated MeDAS Analogs (32−39)[a]

$10 = R^1$: Boc-N-CH$_3$,
$11 = R^1$: Boc-N-CH$_2$CH$_3$,
$12 = R^1$: Boc-N-CH$_2$CH$_2$CH$_3$
$13 = R^1$: Boc-N-CH(CH$_3$)$_2$
$14 = R^1$: Boc-N-CH(CH$_3$)CH$_2$CH$_3$
$15 = R^1$: NO$_2$,

$26 = R^1$: Boc-N-CH$_3$,
$27 = R^1$: Boc-N-CH$_2$CH$_3$,
$28 = R^1$: Boc-N-CH$_2$CH$_2$CH$_3$
$29 = R^1$: Boc-N-CH(CH$_3$)$_2$
$30 = R^1$: Boc-N-CH(CH$_3$)CH$_2$CH$_3$
$31 = R^1$: NO$_2$,

$32 = R^2$: HN-CH$_3$,
$33 = R^2$: HN-CH$_2$CH$_3$,
$34 = R^2$: HN-CH$_2$CH$_2$CH$_3$
$35 = R^2$: HN-CH(CH$_3$)$_2$
$36 = R^2$: HN-CH(CH$_3$)CH$_2$CH$_3$
$37 = R^2$: NH$_2$,

aReagents and condition: (i) NaH (60%), anhydrous DMF, Ar, 0 °C, 4 h, yield 40−80%; (ii) SnCl$_2$, EtOAc:EtOH (3:2), 80 °C, 6 h, yield 30−70%.

Quantitative microPET/CT Imaging. Following radio-labeling, the brain entry, retention, and clearance of each compound was determined by microPET/CT imaging in Sprague−Dawley (SD) rats. For quantitative analysis, the resultant microPET images were registered to the CT images, which allowed us to accurately define the region of interest (ROI) and quantify the radioactivity concentrations of each compound. The radioactivity concentrations were determined in terms of standardized uptake values (SUV). As shown in Figure 4A, all of the compounds entered the brain at early time points with various retention and clearance rates at later time points. Similar to [^{11}C]MeDAS, the radioactivity concentration rapidly reached a peak within 5 min and then decreased to reach a plateau at 40−60 min. Most of the F-18-labeled compounds exhibited a relatively low retention and fast clearance, which suggested either slow interaction with myelin membrane or low binding potency. The two lead candidates (compounds 32 and 35) that were identified through fluorescent tissue staining showed distinct in vivo pharmacokinetics. [^{18}F]32 showed the highest brain uptake at early time points and highest retention at later time points with a clearance rate of 2.62, which suggests a low nonspecific binding. In comparison [^{18}F]35 showed relatively high retention at later time points, but the brain uptake was significantly lower than [^{18}F]32 with a clearance rate of 0.70, which suggests a relatively high nonspecific binding. As shown in Figure 4B, although [^{18}F]36 displayed the second highest retention at later time points, the initial brain uptake was the lowest compared with the rest of the compounds with a clearance rate of 0.30, which suggests poor brain permeability or high nonspecific binding. In addition, due to the highest cLogP value (5.27), [^{18}F]36 displayed very slow washout from the whole brain, indicating it is hardly cleared from the brain once penetrating into the BBB. As shown in Figure 4A, both [^{11}C]MeDAS and [^{18}F]32 showed similar brain entry at early time points. Yet, the clearance of [^{18}F]32 was found to be faster than that of [^{11}C]MeDAS. Overall, among the radiolabeled analogs, [^{18}F]32 clearly stands out as the best lead candidate for in vivo imaging of myelin, which is consistent with in vitro FIR data. Representative microPET/CT images of [^{18}F]32 are shown in Figure 5. A 3D movie of microPET imaging of [^{18}F]32 is shown in Supporting Information.
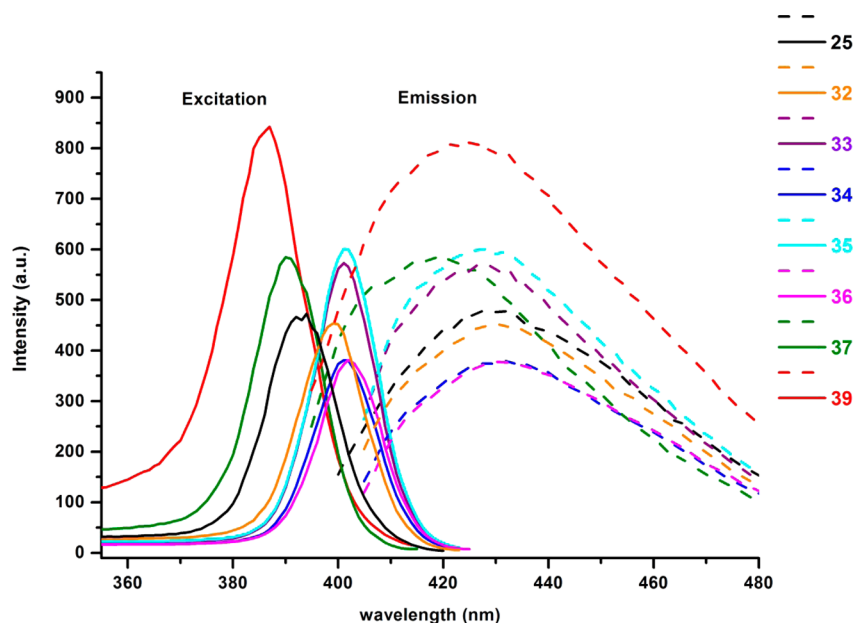
Figure 1. Excitation (Em 420 ± 10 nm; solid) and emission (Ex 390 ± 10 nm; dashed). Spectra of the compounds **25**, **32–37** and **39**.
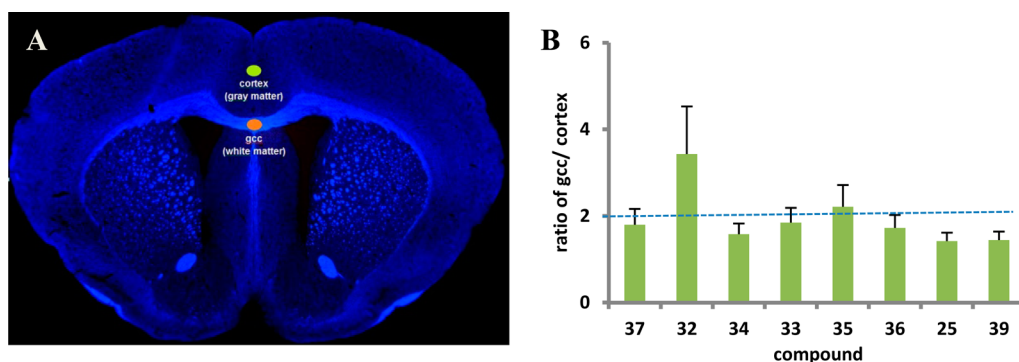

Figure 2. FIR in white matter vs gray matter. (A) Representative in vitro tissue staining showing ROI used for calculation for FIR between white matter and gray matter. (B) ImageJ was used to calculate FIR of each target compound showing compounds **32** and **35** with FIR > 2.
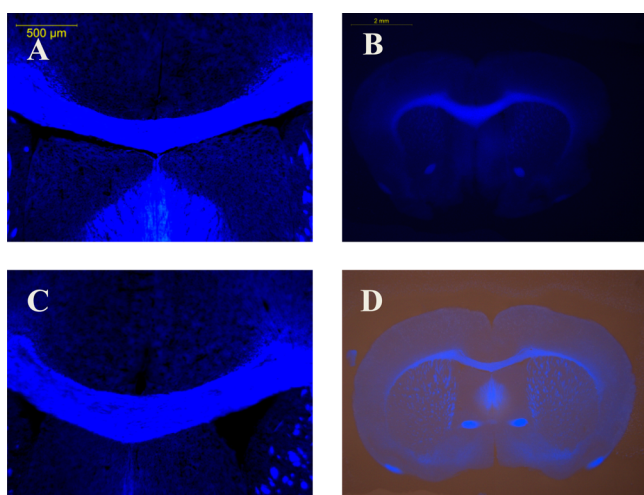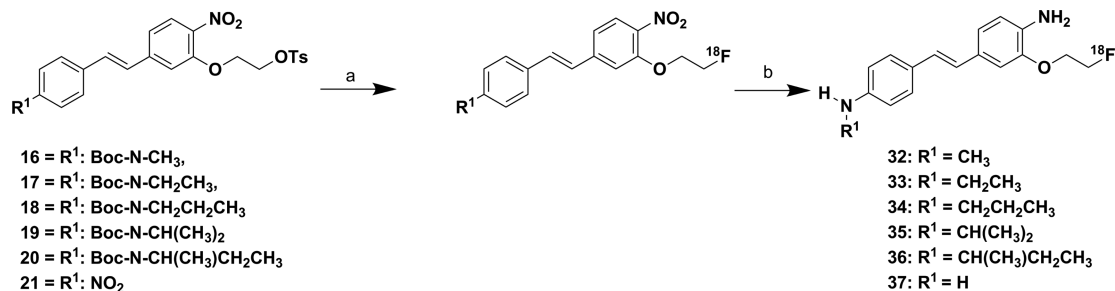

Figure 3. Ex vivo imaging of corpus callosum and the whole brain with compounds (A and B) **32** and (C and D) **35**.

In Situ Autoradiography. To validate the PET results and confirm that the PET signals were indeed from specific binding to myelin, we conducted ex vivo autoradiography. Auto-

radiography allowed us to examine microscopic localization of the radiolabeled compounds after brain entry. After quantitative analysis of microPET/CT studies, [^{18}F]**32** was selected to perform ex vivo film autoradiography, which allowed us to further examine brain permeability and specific binding of the compound. Thus, we conducted ex vivo autoradiography studies in the mouse brain by administering [^{18}F]**32** through tail vein injections. As shown in Figure 6A, [^{18}F]**32** is localized predominantly in the white matter region which is consistent with the pattern of myelin distribution. A relatively distinct labeling of the corpus callosum, an area known to have a high density of myelinated sheaths, was observed after mouse brain tissue sections (coronal) were exposed to film for 10 min. The autoradiographic visualization was consistent with histological staining of myelinated regions (Figure 6C). To demonstrate that radioactivity in the autoradiography was from specific binding to myelin, we pretreated rats with nonlabeled CIC, a myelin-specific agent that we previously developed.[18] As shown in Figure 6B, pretreatment of CIC significantly reduces the contrast of radioactivity in gcc vs cortex. Since CIC itself is also fluorescent, a distinct staining of CIC can be examined on the same section when checked under a fluorescence microscope (Figure 6D). When the film was analyzed using ImageJ, the optical density ratio (ODR) of gcc to cortex was employed to

Scheme 6. Radiosynthesis of Compounds 32−37[a]

16 = R[1]: Boc-N-CH₃,
17 = R[1]: Boc-N-CH₂CH₃,
18 = R[1]: Boc-N-CH₂CH₂CH₃
19 = R[1]: Boc-N-CH(CH₃)₂
20 = R[1]: Boc-N-CH(CH₃)CH₂CH₃
21 = R[1]: NO₂

32: R[1] = CH₃
33: R[1] = CH₂CH₃
34: R[1] = CH₂CH₂CH₃
35: R[1] = CH(CH₃)₂
36: R[1] = CH(CH₃)CH₂CH₃
37: R[1] = H

[a]Reagents and conditions: (a) $^{18}F^-$, K₂CO₃, K₂₂₂, MeCN, 115 °C, 10 min, 60−80%. (b) SnCl₂, EtOH, HCl, 120 °C, 10−20 min, 30−60%.

Scheme 7. Radiosynthesis of Compound 25

1) $^{18}F^-$, K₂CO₃, K₂₂₂, MeCN, 60%

2) SnCl₂, EtOH, HCl, NaOH, 30%

(23)   (25)
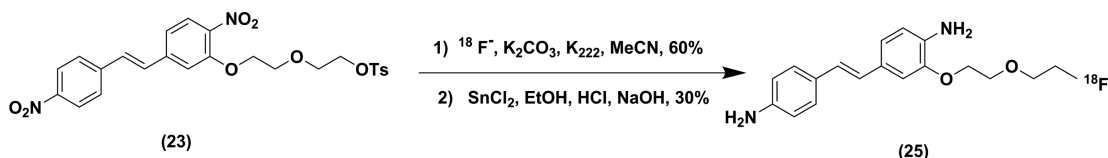
Scheme 8. Radiosynthesis of Compound 39

1) $^{18}F^-$, K₂CO₃, K₂₂₂, MeCN, 60%

2) SnCl₂, EtOH, HCl, NaOH, 30%

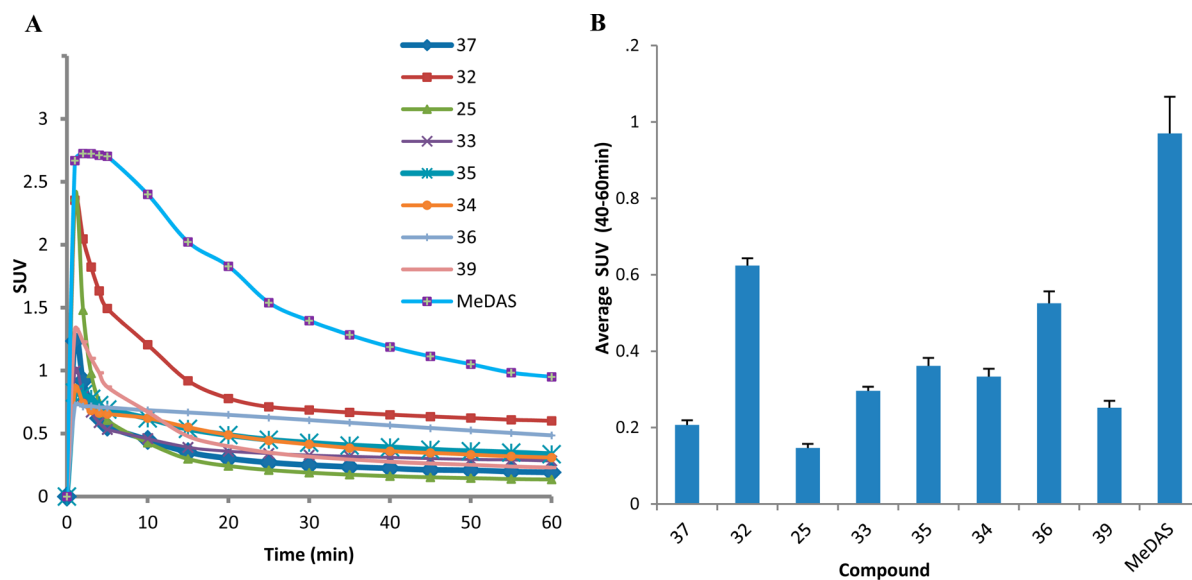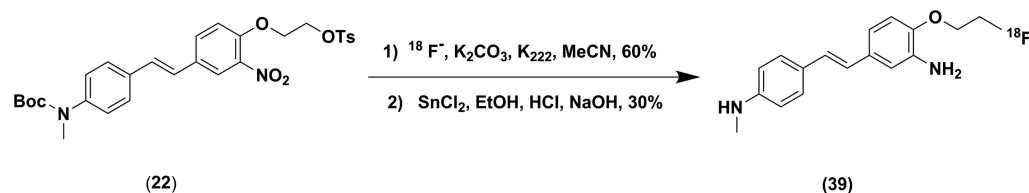(22)   (39)

Figure 4. (A) Average radioactivity concentration of target compounds in the whole brain in terms of SUV as a function of time. (B) Average SUV of late time points (40−60 min).

determine the radiographic staining ratio between white matter and gray matter. Statistical analysis of ODR on the film showed there is a significant difference ($p < 0.05$) between control (3.73 ± 0.31) and ex vivo block studies (1.91 ± 0.04) (Figure 6E). Such an ex vivo competition study suggests that [^{18}F]**32** readily enters the brain and specifically binds to myelin sheaths.

Biostability of [^{18}F]32. Because [^{18}F]**32** showed the highest brain uptake and fastest washout in normal mice, we further evaluated the in vivo biostability of [^{18}F]**32** in plasma.

After injection of [^{18}F]**32**, the plasma samples were harvested and analyzed by radio-HPLC. To the plasma samples were first added ice-cold methanol to precipitate proteins and other biohydrophilic matrix components. The mixtures were centrifuged at 10,000 rpm for 5 min. The supernanent were then separated and loaded onto radio-HPLC for assessment (Phenomenex C-18, 4.6 × 250 mm, acetonitrile:H₂O = 65:35, flow rate of 1 mL/min). Similar to [^{11}C]PIB and [^{18}F]-Flutemetamol,[32] [^{18}F]**32** was rapidly metabolized after tail vein
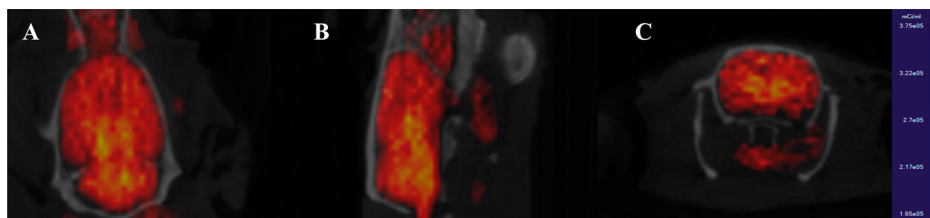
Figure 5. Representative (A) coronal, (B) sagittal, and (C) axial microPET/CT fusion images of the rat brain following i.v. administration of [18F]32, showing high uptakes of [18F]32 in the white matter region of the brain.
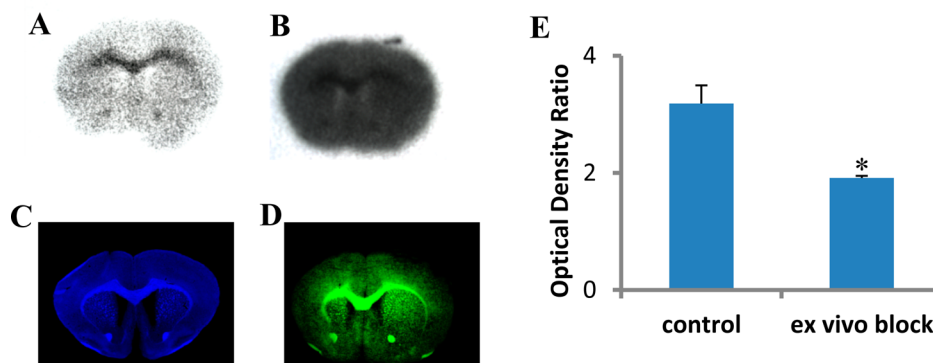

Figure 6. Film autoradiography. (A) Ex vivo autoradiography showing [18F]32 binds to myelinated corpus callosum (CC) in mouse brain (coronal) and was consistent with histological staining of myelinated regions (C). (B) After pretreatment with nonlabeled CIC, ex vivo autoradiographic visualization of CC was significantly decreased. Distinct staining of CIC was observed when the same section was viewed under fluorecent microscope (D). (E) Statistical analysis of optical desity ratio of gcc to cortex on the film showed there is significant diffrence between control and ex vivo or in vitro block studies. *: $p < 0.05$.

injection. The percentage of parent [18F]32 in plasma was determined to be $78.14 \pm 9.15\%$ at 5 min after injection. The percentage of parent [18F]32 decreased to $53.12 \pm 7.31\%$ and $32.45 \pm 5.80\%$ at 30 and 60 min postinjection. All the metabolites found in the plasma were hydrophilic with retention time close to void volume, which are incapable of penetrating the BBB.

◼ CONCLUSION

A series of fluorinated myelin-imaging agents can be F-18 labeled for PET imaging of myelin. Structure−activity relationship studies showed that selected lead compounds exhibit cLogP values in the range of 3−4. Compounds with a shorter alkyl chain such as methyl showed higher permeability across the BBB than those with a longer or branched alkyl chain. Through a series of in vitro, ex vivo, and in vivo assays, we identified a lead candidate that is suitable for PET imaging of myelin. Further studies are under way to explore the potential of compound 32 as an imaging marker for efficacy evaluation of therapeutic drugs currently under development.

◼ EXPERIMENTAL SECTION

General Procedures. All chemicals and reagents were used as received without further purification. Glassware was dried in an oven at 130 °C and purged with a dry atmosphere prior to use. Unless otherwise mentioned, reactions were performed open to air. Reactions were monitored by TLC and visualized by a dual short/long wavelength UV lamp. Flash column chromatography was performed using 230−400 mesh silica gel (Fisher). NMR spectra were recorded on a Varian Inova 400 spectrometer and a 500 MHz Bruker Ascend Avance III HD at room temperature. Chemical shifts for ^{1}H and ^{13}C NMR were reported as δ, part per million (ppm), and referenced to an internal deuterated solvent central line. Multiplicity and coupling constants (J) were calculated automatically on MestReNova 10.0, a

NMR processing software from Mestrelab Research. The purity of the newly synthesized compounds as determined by analytical HPLC was >95% on C-18 reversed-phase HPLC (Phenomenex, 10 × 250 mm), eluent: acetonitrile:H_2O = 60:40, flow rate of 3.0 mL/min. HRMS-ESI mass spectra were acquired on an Agilent Q-TOF. Fluorescence was measured with a Cary Eclipse spectrophotometer using 1 × 1 cm quartz cuvette in a 10 mM acetonitrile solution.

General Method for Synthesis. 3-Hydroxy-4-nitrobenzaldehyde (1) or 4-hydroxy-3-nitrobenzaldehyde (2) (1.5 g, 8.9 mmol) was deprotonated with K_2CO_3, (2.48 g, 17.9 mmol) in 20 mL DMF followed by dropwise adding alkylene glycol ditosylate (a-b, 1 equiv) dissolved in 10 mL DMF at 80 °C. The reaction mixtures were heated with continuous stirring for additional 6 h. After completion of the reactions, the mixtures were cooled to room temperature, after 30 min, 200 mL ice cold water added, and extracted with 3 × 50 mL ethyl acetate. The organic phases were combined and washed with 20% sodium bicarbonate (50 mL), 50 mL brine, dried over $MgSO_4$, and evaporated under reduced pressure. The crude products were purified by flash column chromatography in an ethyl acetate−hexane mixture.

2-(5-Formyl-2-nitrophenoxy)ethyl 4-Methylbenzenesulfonate (3). This dull yellow crystalline solid was eluted in 40% EtOAc:hexane, yield 1.2 g, (60%). ^{1}H NMR (400 MHz, chloroform-*d*) δ 10.07 (s, 1H), 7.95 (d, J = 8.1 Hz, 1H), 7.84 (d, J = 8.4 Hz, 2H), 7.62 (dd, J = 8.1, 1.5 Hz, 1H), 7.56 (d, J = 1.5 Hz, 2H), 7.41 (dq, J = 7.9, 0.7 Hz, 2H), 4.45 (d, J = 1.4 Hz, 4H), 2.49 (s, 3H). ^{13}C NMR (101 MHz, chloroform-*d*) δ 190.2, 151.6, 145.5, 139.7, 132.5, 130.2, 128.2, 126.3, 123.6, 113.9, 67.6, 67.3, 21.9.

2-(2-(5-Formyl-2-nitrophenoxy)ethoxy)ethyl 4-Methylbenzenesulfonate (4). The off white crystalline compound was eluted in 30% EtOAc:hexane, yield 1.0 g, (40%). ^{1}H NMR (400 MHz, chloroform-*d*) δ 10.02 (s, 1H), 7.90 (d, J = 8.2 Hz, 1H), 7.76 (d, J = 8.3 Hz, 2H), 7.59 (d, J = 1.5 Hz, 1H), 7.54 (d, J = 8.1 Hz, 1H), 7.31 (dt, J = 8.0, 0.7 Hz, 1H), 4.32−4.21 (m, 2H), 4.20−4.11 (m, 2H), 3.87−3.80 (m, 2H), 3.78−3.71 (m, 2H), 2.41 (s, 3H). ^{13}C NMR (101 MHz, chloroform-*d*) δ 190.5, 152.5, 145.1, 139.8, 133.1, 130.0, 128.1, 126.1, 122.9, 114.5, 70.1, 69.5, 69.4, 21.9.

3-(2-Fluoroethoxy)-4-nitrobenzaldehyde (5). 3-Hydroxy-4-nitro-benzaldehyde (**1**, 1.0 g, 6.0 mmol) was deprotonated with K_2CO_3 (1.65 g, 12.0 mmol) in 10 mL dry DMF followed by reaction with 1-fluoro-2-iodoethane (0.8 mL, 9.0 mmol, 2.14 g/mL) at 80 °C.[29] The reaction was monitored by TLC, and after 6 h no starting material was detected. The reaction mixture was cooled to room temperature, 100 mL ice cold water was added, and the compound was precipitated out, filtered under vacuum, and washed with water and diethyl ether. A yellow amorphous compound was obtained [yield 0.90 g, (70%)] and used without further purification for the next reaction. ^{1}H NMR (400 MHz, chloroform-*d*) δ 10.05 (s, 1H), 7.94 (d, *J* = 7.6 Hz, 1H), 7.69–7.54 (m, 2H), 4.82 (d, *J* = 47.5 Hz, 2H,), 4.45 (d, *J* = 27.0 Hz, 2H,). ^{13}C NMR (101 MHz, CDCl₃) δ 190.3, 139.8, 126.7(2C), 123.6(2C), 114.0, 81.4 (d, J_{C-F} = 173 Hz), 69.4 (d, J_{C-F} = 21 Hz). ^{19}F NMR (376 MHz, CDCl₃) δ −90.90 − −91.16 (C−F coupling) −100.01 (F-decoupling).

2-(4-Formyl-2-nitrophenoxy)ethyl 4-Methylbenzenesulfonate (6). The white crystalline compound was eluted in 40% EtOAc:hexane, yield 0.45 g (65%). ^{1}H NMR (400 MHz, chloroform-*d*) δ 9.93 (s, 1H), 8.32 (d, *J* = 2.1 Hz, 1H), 8.01 (dd, *J* = 8.8, 2.4 1H), 7.78 (d, *J* = 8.3 Hz, 2H), 7.32 (dd, *J* = 8.4, 0.8 Hz, 2H), 7.18 (d, *J* = 8.7 Hz, 1H), 4.57−4.30 (m, 4H), 2.45 (s, 3H). ^{13}C NMR (101 MHz, chloroform-*d*) δ 188.8, 155.6, 145.6, 134.9, 132.3, 130.3, 129.8, 128.1, 127.5, 114.9, 67.7, 67.2, 21.9.

4-(2-Fluoroethoxy)-3-nitrobenzaldehyde (7). The off white amorphous compound was precipitated out and was used without further purification, yield 1.1 g (86%). ^{1}H NMR (400 MHz, chloroform-*d*) δ 9.95 (s, 1H), 8.36 (dd, *J* = 2.1, 0.8 Hz, 1H), 8.08 (ddd, *J* = 8.7, 2.0, 0.6 Hz, 1H), 7.27−7.25 (m, 1H), 4.94−4.86 (m, 1H), 4.81−4.73 (m, 1H), 4.55−4.40 (m, 2H). ^{13}C NMR (101 MHz, chloroform-*d*) δ 188.9, 156.2, 134.8, 129.8, 127.7, 115.0, 82.2, 80.4, 69.5, 69.3. ^{19}F NMR (376 MHz, chloroform-*d*) δ −90 − −91.13(m), −100.01 (s).

tert-Butyl (4-((Diethoxyphosphoryl)methyl)phenyl)carbamate (9). Compound **9** was synthesized according to our earlier published method.[28] To a 100 mL round-bottom flask with a magnetic stir bar, diethyl 4-aminobenzylphosphonate (**8**, 5.0 g, 20.56 mmol), di-*tert*-butyl dicarbonate (4.50 g, 21.0 mmol), THF (25 mL), and water (10 mL) were added. The reaction was stirred at room temperature open to air overnight. After completion of the reaction, THF was evaporated under vacuum, and the resulting residue was diluted with water and extracted with ethyl acetate (50 mL × 3) three times. The organic layers were combined and washed twice with water (50 mL × 2) and once with brine (50 mL). The organic layer was dried over MgSO₄, filtered, and evaporated under reduced pressure. The resulting white amorphous compound was obtained [yield 6.5 g (95%)] and used without further purification.[28] ^{1}H NMR (400 MHz, chloroform-*d*) δ 7.30 (br d, *J* = 8.4 Hz, 2H), 7.17−7.19 (m, 2H), 6.87 (br s, 1H), 4.04−3.91 (m, 4H), 3.07 (d, $^2J_{H,P}$ = 21.2 Hz, 2H), 1.49 (s, 9H), 1.22 (td, $^3J_{H,H}$ = 6.8 Hz, $^4J_{H,P}$ = 0.4 Hz, 6H). ^{13}C NMR (100 MHz, chloroform-*d*) δ 152.8, 137.4, 130.1, 125.5, 118.4, 80.3, 62.0, 32.9 (d, $^1J_{C,P}$ = 138 Hz, 1C), 28.8, 16.3.

General Method for Alkylation of *tert*-Butyl (4-((Diethoxyphosphoryl)methyl)phenyl)carbamate (10−14). To an oven-dried 100 mL round-bottom flask purged with argon gas and fitted with a magnetic stirrer were added sodium hydride (0.150 g, 5.82 g, 95%) and *tert*-butyl (4-((diethoxyphosphoryl)methyl)phenyl)-carbamate (**9**, 1.0 g, 2.9 mmol). The mixture was purged with argon gas, and dry THF (25 mL) at 0 °C was added. Iodo-alkane (4.0 equiv) was added dropwise after 30 min at 0 °C under argon gas. The reaction was stirred under argon and allowed to reach room temperature overnight. After completion, the reaction was quenched with water, and THF was removed by vacuum. The residue was dissolved in dichloromethane (DCM) and water, and the aqueous layer was extracted three times with DCM (30 mL × 3). The organic layers were combined and washed twice with water (50 mL × 2) and once with brine (50 mL). The organic layer was dried over MgSO4 and then filtered and concentrated to yield the desired products **10−14** as sticky oil. This was purified over a silica flash column using hexane:ethyl acetate as eluent as required with derivatives.

tert-Butyl (4-((Diethoxyphosphoryl)methyl)phenyl)(methyl)-carbamate (10). This dark yellow sticky oil was used without further purification, yield 0.80 g, (76%).[28] ^{1}H NMR (400 MHz, chloroform-*d*) δ 7.24−7.25 (m, 2H), 7.16 (d, *J* = 8.0 Hz, 2H), 4.07−3.94 (m, 4H), 3.22 (s, 3H), 3.11 (d, $^3J_{H,P}$ = 21.6 Hz, 2H), 1.42 (s, 9H), 1.23 (t, *J* = 7.2, 6H). ^{13}C NMR (100 MHz, chloroform-*d*) δ 154.5, 142.4, 129.7, 128.4, 125.4, 80.1, 61.9, 37.1, 33.0 (d, $^2J_{C,P}$ = 138 Hz, 1C), 28.1, 16.3.

tert-Butyl (4-((diethoxyphosphoryl)methyl)phenyl)(ethyl)-carbamate (11). This clear sticky oil was eluted in 30% EtOAc:hexane, yield 0.65 g (40%). ^{1}H NMR (400 MHz, chloroform-*d*) δ 7.28−7.23 (m, 2H), 7.11 (d, *J* = 8.0 Hz, 2H), 4.00 (dqd, *J* = 8.3, 7.1, 3.7 Hz, 4H), 3.64 (q, *J* = 7.1 Hz, 2H), 3.13 (d, $J_{H,P}$ = 21.6 Hz, 2H), 1.40 (s, 9H), 1.23 (td, *J* = 7.1, 0.4 Hz, 6H), 1.11 (t, *J* = 7.1 Hz, 3H). ^{13}C NMR (101 MHz, chloroform-*d*) δ 141.0, 129.9, 129.8, 129.0, 128.9, 126.9, 79.7, 62.0, 61.9, 44.6, 33.1 (d, $J_{C,P}$ = 138 Hz, 1C), 28.1, 16.2, 16.2, 13.6.

tert-Butyl (4-((Diethoxyphosphoryl)methyl)phenyl)(propyl)-carbamate (12). This clear sticky oil was eluted in 30% EtOAc:hexane, yield 0.400 g, (25%). ^{1}H NMR (400 MHz, chloroform-*d*) δ 7.23 (d, *J* = 2.5 Hz, 1H), 7.21 (d, *J* = 2.6 Hz, 1H), 7.08 (d, *J* = 8.0 Hz, 2H), 3.97 (dqd, *J* = 8.3, 7.1, 3.9 Hz, 4H), 3.57−3.47 (m, 2H), 3.10 (d, $J_{H,P}$ = 21.6 Hz, 2H), 1.54−1.45 (m, 2H), 1.37 (s, 9H), 1.22−1.17 (m, 6H), 0.83 (t, *J* = 7.4 Hz, 3H). ^{13}C NMR (101 MHz, chloroform-*d*) δ 141.3, 141.2, 130.0, 129.9, 128.0, 127.1, 127.0, 127.0, 79.8, 62.1, 62.0, 51.5, 33.2 (d, $J_{C,P}$ = 138 Hz, 1C), 28.2, 21.5, 16.3, 16.2, 11.0.

tert-Butyl (4-((Diethoxyphosphoryl)methyl)phenyl)(isopropyl)-carbamate (13). This yellow Oil was eluted in 25% EtOAc:hexane, yield 0.41 g (25%). ^{1}H NMR (400 MHz, chloroform-*d*) δ 7.24 (dd, *J* = 7.8, 2.0 Hz, 2H), 6.97 (d, *J* = 8.0 Hz, 2H), 4.56−4.41 (m, 1H), 4.02−3.89 (m, 4H), 3.12 (d, $J_{H,P}$ = 21.6 Hz, 2H), 1.31 (s, 9H), 1.18 (td, *J* = 7.1, 0.6 Hz, 6H), 1.03 (dd, *J* = 6.8, 0.8 Hz, 6H). ^{13}C NMR (101 MHz, chloroform-*d*) δ 130.1, 130.0, 129.8, 129.8, 129.7, 79.4, 62.0, 62.0, 33.2 (d, $J_{C,P}$ = 138 Hz, 1C), 28.1, 21.2, 16.2, 16.2.

tert-Butyl sec-Butyl(4-((diethoxyphosphoryl)methyl)phenyl)-carbamate (14). This clear oil was eluted in 30% EtOAc:hexane, yield 0.20 g (15%). ^{1}H NMR (400 MHz, chloroform-*d*) δ 7.29−7.25 (m, 2H), 7.08−6.98 (m, 2H), 4.21 (d, *J* = 10.3 Hz, 1H), 4.06−3.92 (m, 4H), 3.14 (d, $J_{H,P}$ = 21.6 Hz, 2H), 1.54 (dt, *J* = 13.5, 7.5 Hz, 1H), 1.35 (s, 9H), 1.28 (d, *J* = 7.1 Hz, 1H), 1.26−1.17 (m, 6H), 1.05 (d, *J* = 6.9 Hz, 3H), 0.95 (t, *J* = 7.4 Hz, 3H). ^{13}C NMR (101 MHz, CDCl₃) δ 154.9, 138.1, 129.9, 129.8, 129.7, 129.6, 129.6, 129.5, 129.5, 79.3, 62.0, 61.9, 54.3, 33.2 (d, $J_{C,P}$ = 138 Hz, 1C), 28.2, 28.1, 19.1, 16.2, 16.1, 11.2.

General Method for the Synthesis of 16−22 (Scheme 3). To an oven-dried 100 mL round-bottom flask purged with argon and fitted with a magnetic stirrer was added sodium hydride (2.0 eq., 60% dispersion in mineral oil). The flask was purged with argon, and dry DMF 2.0 mL was added. The compound (**10−15**, 1.1 equiv) was dissolved in dry DMF (2.0 mL) and transferred via syringe in a NaH-DMF mixture to a flask. The mixture was stirred under argon at 0 °C for 1 h. **3** or **6** (1.0 equiv) was dissolved in dry DMF (2 mL) and added to the reaction mixture via syringe under argon at 0 °C. The reaction was stirred for 2 h at 0 °C in the dark under argon. The reaction was quenched with water (25 mL) and extracted with ethyl acetate (30 mL × 3) three times. The organic layers were combined and washed with water (25 mL × 2) twice and once with brine (25 mL). The organic layer was dried over MgSO₄, filtered, and concentrated to give sticky oil as crude product. This was purified by dissolving in a minimal amount of DCM and made slurry with silica gel and dried under vacuum. The compound was eluted in 10−15% ethyl acetate:hexane in a flash column.

(E)-2-(5-(4-((tert-Butoxycarbonyl)(methyl)amino)styryl)-2-nitrophenoxy)ethyl-4-methylbenzenesulfonate (16). This yellow amorphous compound was eluted in 15% EtOAc:hexane, yield 0.140 g (40%). ^{1}H NMR (400 MHz, chloroform-*d*) δ 7.88 (d, *J* = 8.5 Hz, 1H), 7.84−7.80 (m, 2H), 7.50 (d, *J* = 8.5 Hz, 2H), 7.37−7.33 (m, 2H), 7.29 (d, *J* = 8.4 Hz, 2H), 7.22−7.19 (m, 1H), 7.18−7.16 (m, 1H), 7.11 (d, *J* = 1.7 Hz, 1H), 6.99 (d, *J* = 16.3 Hz, 1H), 4.41 (q, *J* = 2.1 Hz, 4H), 3.29 (s, 3H), 2.44 (s, 3H), 1.48 (s, 9H). ^{13}C NMR (101

MHz, chloroform-*d*) δ 145.4, 144.5, 144.2, 132.8, 130.2, 128.2, 127.4, 126.7, 125.9, 125.6, 119.4, 113.0, 67.8, 37.3, 28.5, 21.9.

(E)-2-(5-(4-((tert-Butoxycarbonyl)(ethyl)amino)styryl)-2-nitrophenoxy)ethyl-4-methylbenzenesulfonate (17). The yellow sticky solid product was eluted in a silica flash column with 15% EtOAc:hexane. The yellow amorphous product yield 0.125 (40%). ^{1}H NMR (400 MHz, chloroform-*d*) δ 7.87 (d, *J* = 8.5 Hz, 1H), 7.84−7.80 (m, 2H), 7.50 (d, *J* = 8.5 Hz, 2H), 7.38−7.33 (m, 2H), 7.24 (d, *J* = 8.5 Hz, 2H), 7.22−7.19 (m, 1H), 7.18−7.16 (m, 1H), 7.11 (d, *J* = 1.7 Hz, 1H), 7.00 (d, *J* = 16.3 Hz, 1H), 4.48−4.35 (m, 4H), 3.70 (q, *J* = 7.1 Hz, 2H), 2.44 (s, 3H), 1.46 (s, 9H), 1.17 (t, *J* = 7.1 Hz, 3H). ^{13}C NMR (101 MHz, chloroform-*d*) δ 152.3, 145.4, 144.1, 143.1, 133.5, 132.7, 132.5, 130.1, 128.1, 127.4, 127.1, 126.7, 126.0, 119.3, 112.9, 80.50, 67.7, 67.6, 45.0, 28.5, 21.8, 14.1.

(E)-2-(5-(4-((tert-Butoxycarbonyl)(propyl)amino)styryl)-2-nitrophenoxy)ethyl-4-methylbenzenesulfonate (18). The yellow crystalline compound was eluted on a silica flash column in 15% EtOAc:hexane. Yield 0.165 g (35%). ^{1}H NMR (400 MHz, chloroform-*d*) δ 7.87 (d, *J* = 8.5 Hz, 1H), 7.85−7.79 (m, 2H), 7.50 (d, *J* = 8.4 Hz, 2H), 7.35 (dt, *J* = 7.9, 0.7 Hz, 2H), 7.23 (d, *J* = 8.4 Hz, 2H), 7.21−7.19 (m, 1H), 7.18−7.16 (m, 1H), 7.11 (d, *J* = 1.7 Hz, 1H), 7.00 (d, *J* = 16.2 Hz, 1H), 4.46−4.37 (m, 4H), 3.67−3.57 (m, 2H), 2.44 (s, 3H), 1.60 (s, 1H), 1.57 (s, 1H), 1.45 (s, 9H), 0.89 (t, *J* = 7.4 Hz, 3H). ^{13}C NMR (101 MHz, chloroform-*d*) δ 152.3, 145.4, 144.1, 133.5, 132.7, 132.5, 130.1, 128.1, 127.4, 127.3, 126.7, 126.0, 119.3, 112.9, 80.5, 67.7, 67.6, 51.6, 28.5, 21.9, 21.8, 11.3.

(E)-2-(5-(4-((tert-Butoxycarbonyl)(isopropyl)amino)styryl)-2-nitrophenoxy)ethyl-4-methylbenzenesulfonate (19). The yellow amorphous compound was eluted on a silica flash column in 15% EtOAc:hexane, yield 0.065 g (30%). ^{1}H NMR (500 MHz, chloroform-*d*) δ 7.87 (dd, *J* = 8.5, 2.0 Hz, 1H), 7.84−7.79 (m, 2H), 7.53−7.48 (m, 2H), 7.35 (d, *J* = 7.8 Hz, 2H), 7.23−7.17 (m, 2H), 7.14−7.09 (m, 3H), 7.06−7.00 (m, 1H), 4.57−4.46 (m, 1H), 4.42 (h, *J* = 4.3, 3.7 Hz, 4H), 2.44 (s, 3H), 1.39 (s, 9H), 1.13 (dd, *J* = 6.9, 2.0 Hz, 6H). ^{13}C NMR (126 MHz, chloroform-*d*) δ 154.9, 152.4, 145.4, 144.1, 140.2, 138.8, 134.8, 132.8, 132.6, 130.5, 130.2, 128.2, 127.3, 126.7, 126.5, 119.5, 113.1, 80.1, 67.8, 67.8, 28.6, 21.9, 21.8.

(E)-2-(5-(4-((tert-Butoxycarbonyl)(sec-butyl)amino)styryl)-2-nitrophenoxy)ethyl-4-methylbenzenesulfonate (20). The yellow sticky solid was eluted in 10% EtOAc:hexane, yield 0.040 g (15%). ^{1}H NMR (400 MHz, chloroform-*d*) δ 7.88 (d, *J* = 8.5 Hz, 1H), 7.85−7.80 (m, 2H), 7.53−7.49 (m, 2H), 7.37−7.33 (m, 2H), 7.23−7.20 (m, 1H), 7.18 (d, *J* = 1.9 Hz, 1H), 7.15−7.10 (m, 3H), 7.02 (d, *J* = 16.3 Hz, 1H), 4.45−4.38 (m, 4H), 4.23 (d, *J* = 7.0 Hz, 1H), 2.44 (s, 3H), 1.67−1.58 (m, 1H), 1.40 (s, 9H), 1.37−1.32 (m, 1H), 1.12 (d, *J* = 6.8 Hz, 3H), 0.98 (t, *J* = 7.4 Hz, 3H). ^{13}C NMR (101 MHz, chloroform-*d*) δ 152.3, 145.4, 144.0, 134.6, 132.7, 132.5, 130.2, 130.1, 130.1, 128.1, 127.2, 126.7, 126.4, 119.4, 113.0, 80.1, 67.7, 67.7, 66.8, 55.2, 28.7, 28.5, 21.8, 19.7, 11.6.

(E)-2-(2-Nitro-5-(4-nitrostyryl)phenoxy)ethyl-4-methylbenzenesulfonate (21). A yellow amorphous precipitate formed after quenching with water and was then washed several times with water and diethyl ether. The yellow amorphous product yield was 0.150 g (75%). ^{1}H NMR (400 MHz, DMSO-*d*$_6$) δ 8.31−8.25 (m, 2H), 7.93 (d, *J* = 8.4 Hz, 1H), 7.91−7.86 (m, 2H), 7.79−7.74 (m, 2H), 7.65 (d, *J* = 16.5 Hz, 1H), 7.60−7.52 (m, 2H), 7.42 (t, *J* = 8.2 Hz, 3H), 4.50−4.34 (m, 4H), 2.39 (s, 3H). ^{13}C NMR (101 MHz, DMSO) δ 151.7, 147.4, 145.7, 143.7, 143.2, 139.1, 132.6, 131.7, 131.1, 130.8, 128.5, 128.4, 128.2, 128.1, 126.5, 126.5, 124.8, 124.8, 124.7, 120.4, 113.6, 69.2, 67.6, 21.8.

(E)-2-(5-(4-((tert-Butoxycarbonyl)(methyl)amino)styryl)-2-nitrophenoxy)ethyl-4-methylbenzenesulfonate (22). The yellow crystalline compound was purified over a silica flash column in 20% EtOAc:hexane, yield 0.240 g (50%). ^{1}H NMR (500 MHz, chloroform-*d*) δ 7.96 (s, 1H), 7.82 (d, *J* = 8.1 Hz, 2H), 7.62 (dd, *J* = 8.6, 2.2 Hz, 1H), 7.46 (d, *J* = 8.3 Hz, 2H), 7.37 (d, *J* = 8.1 Hz, 2H), 7.27 (s, 2H), 7.07−7.02 (m, 2H), 6.97 (d, *J* = 16.3 Hz, 1H), 4.45−4.33 (m, 4H), 3.29 (s, 3H), 2.46 (s, 3H), 1.49 (s, 9H). ^{13}C NMR (126 MHz, chloroform-*d*) δ 154.5, 150.3, 145.1, 143.6, 133.2, 132.3, 131.5, 129.9,

129.3, 127.8, 126.6, 125.4, 125.0, 122.9, 115.3, 80.5, 67.4, 67.4, 37.0, 28.2, 21.6.

Synthesis of (E)-2-(2-(2-Nitro-5-(4-nitrostyryl)phenoxy)ethyl-4-methylbenzene-sulfonate 23 (Scheme 4). To an oven-dried 100 mL round-bottom flask purged with argon and fitted with a magnetic stirring bar was added sodium hydride (0.80 g, 2.0 mmol, 60% dispersion in mineral oil). The flask was purged with argon, and dry DMF 2.0 mL was added. The diethyl (4-nitrobenzyl) phosphonate (**15**, 0.30 g, 1.1 mmol) was dissolved in dry DMF (2.0 mL), and the NaH-DMF mixture was transferred via syringe to a flask. The mixture was then stirred under argon at 0 °C for 1 h. The tosylated 4-nitrobenzaldehyde (**4**, 0.360 g 1.0 mmol) was dissolved in dry DMF (2 mL) and added to the reaction mixture via syringe under argon at 0 °C. The reaction was stirred again for 2 h at 0 °C in the dark under argon. The reaction was quenched with 25 mL of ice cold water, and the compound precipitated out. It was then filtered under vacuum, washed with water several times followed by diethyl ether, and used for the next step without further purification. The yellow amorphous compound was dried under high vacuum, yield 0.390 g (80%). ^{1}H NMR (400 MHz, DMSO-*d*$_6$) δ 8.31−8.25 (m, 2H), 7.95 (d, *J* = 8.4 Hz, 1H), 7.92−7.87 (m, 2H), 7.79−7.74 (m, 2H), 7.68 (d, *J* = 16.5 Hz, 1H), 7.64−7.55 (m, 2H), 7.42 (dd, *J* = 9.1, 3.0 Hz, 3H), 4.30 (t, *J* = 4.6 Hz, 2H), 4.19−4.09 (m, 2H), 3.79−3.62 (m, 4H), 2.37 (s, 3H). ^{13}C NMR (101 MHz, DMSO) δ 151.8, 146.7, 144.8, 143.1, 142.6, 138.5, 132.3, 131.2, 130.4, 130.1, 127.8, 127.6, 125.9, 124.2, 119.4, 113.1, 70.0, 69.1, 68.5, 68.2, 21.1.

(E)-2-(2-(2-Fluoroethoxy)ethoxy)-1-nitro-4-(4-nitrostyryl)benzene (24). Compound (**23**, 0.15 g, 0.28 mmol) and Kryptofix 2.2.2. (K$_{222}$, 0.33 g, 0.85 mmol) with CsF (0.09 g, 0.57 mmol) as the source of fluoride-19 were mixed together in a 100 mL round-bottom flask in dry acetonitrile (20 mL), and the reaction was purged with argon. The reaction mixture was heated at 80 °C for 4 h and monitored by TLC. Once the reaction was complete, acetonitrile was evaporated under reduced pressure, and the reaction was quenched with ice cold water. The dark brown precipitate was filtered under vacuum and washed with water several times and diethyl ether once. The light brown amorphous product yield was 0.090 g, and 84% was used with further purification. ^{1}H NMR (400 MHz, chloroform-*d*) δ 8.26 (d, *J* = 8.3 Hz, 2H), 7.92 (d, *J* = 8.0 Hz, 1H), 7.68 (d, *J* = 8.5 Hz, 2H), 7.29 (d, *J* = 1.6 Hz, 1H), 7.25−7.18 (m, 3H), 4.60 (dt, *J* = 47.8, 4.0 Hz, 2H), 4.37 (t, *J* = 4.7 Hz, 2H), 3.99 (t, *J* = 4.6 Hz, 2H), 3.88 (dt, *J* = 30.1, 3.8 Hz, 3H). ^{13}C NMR (101 MHz, chloroform-*d*) δ 170.4, 156.3, 153.2, 136.1, 135.6, 134.5, 131.1, 131.1, 131.0, 130.5, 127.7, 127.6, 126.7, 124.5, 119.4, 117.5, 113.6, 105.3, 94.6, 86.6 (d, *J*$_{C−F}$ = 164 Hz), 70.1 (*J*$_{C−F}$, *J* = 43 Hz). ^{19}F NMR (376 MHz, chloroform-*d*) δ −100.01.

(E)-4-(4-Aminostyryl)-2-(2-(2-fluoroethoxy)ethoxy)aniline (25). To a 100 mL round-bottom flask with a magnetic stirring bar was added tin(II) chloride (0.285 g, 1.5 mmol). (*E*)-2-(2-(2-fluoroethoxy)-ethoxy)-1-nitro-4-(4-nitrostyryl)benzene (**24**, 0.050 g, 0.15 mmol) was added to the tin(II) chloride solution of ethyl acetate (15 mL) and ethanol (10 mL). The reaction mixture was refluxed under a water-cooled condenser in an oil bath at 70 °C and stirred overnight open to air. The reaction was monitored via TLC and after completion of the reaction was cooled to room temperature, and the solvent was removed by vacuum. The compound was dissolved in aq Na$_2$CO$_3$ (20%) until bubbles stopped forming and was washed with ethyl acetate 3 times (30 mL × 3), water (50 mL × 2), followed by brine (50 mL). The organic layer was dried over the MgSO$_4$, filtered, and concentrated to give the crude **25**. The crude product was dissolved in minimal DCM and purified on silica by flash column chromatography with a mobile phase of EtOAc:hexane, and **25** was eluted in 10−15% EtOAc:hexane yielding a sticky brown solid, yield 0.02 g, (49%). ^{1}H NMR (400 MHz, chloroform-*d*) δ 7.28−7.24 (m, 2H), 6.95 (d, *J* = 1.8 Hz, 1H), 6.90 (dd, *J* = 8.0, 1.8 Hz, 1H), 6.78 (s, 2H), 6.66−6.63 (m, 2H), 6.62 (d, *J* = 1.9 Hz, 1H), 4.68−4.61 (m, 1H), 4.57−4.49 (m, 1H), 4.27−4.15 (m, 2H), 3.90−3.86 (m, 2H), 3.86−3.80 (m, 2H), 3.79−3.72 (m, 3H). ^{13}C NMR (101 MHz, chloroform-*d*) δ 146.2, 145.3, 136.1, 128.61, 128.4, 127.1, 125.3, 125.0, 120.4, 115.1, 115.0, 110.1, 81.8 (d, *J*$_{C−F}$ = 171 Hz), 69.4 (d, *J*$_{C−F}$ = 21.0 Hz). ^{19}F NMR (376 MHz, chloroform-*d*) δ −89.8 − −90.7 (m), −100.0.

General Method for the Synthesis of 26–31 (Scheme 5, Step (i)). To an oven-dried 100 mL round-bottom flask with a magnetic stirring bar was added sodium hydride (NaH, 2.0 equiv, 60%). The flask was purged with argon, and 2.0 mL dry DMF was added. The solution was stirred under argon in an ice bath (0 °C). Boc-N-R[1]-diethyl benzoylphosphonate and diethyl (4-nitrobenzyl)phosphonate (**10–15**, 1.2 equiv) in 2.0 mL dry DMF were added to the solution of NaH. This sodium hydride and intermediate (**10–15**) mixture was stirred at 0 °C under argon for 1 h. Then 2.0 mL dry DMF solution of fluorinated nitrobenzaldehyde (**5, 7**) was transferred via syringe to the reaction mixture under argon at 0 °C. The reaction was continued for another 2 h at 0 °C under argon and monitored via TLC. Once completed, the reaction was quenched with ice cold water (50 mL) and extracted with ethyl acetate (50 mL × 3) three times. The organic layer was washed twice with water (50 mL × 2) and once with brine (50 mL). The organic layer was dried over MgSO$_4$, filtered, and concentrated to give a yellow crude solid/oil. The solid was dissolved in 2 mL ethyl acetate and loaded onto a silica column and eluted with ethyl acetate and hexane.

tert-Butyl (E)-(4-(3-(2-Fluoroethoxy)-4-nitrostyryl)phenyl)-(methyl)carbamate (26). This yellow amorphous compound was purified on a silica flash column in 15% EtOAc:hexane, yield 0.080 g, (30%). ^{1}H NMR (400 MHz, chloroform-d) δ 7.91–7.86 (m, 1H), 7.47 (d, J = 8.1 Hz, 2H), 7.27 (d, J = 8.1 Hz, 2H), 7.19 (d, J = 7.2 Hz, 1H), 7.14 (d, J = 2.9 Hz, 2H), 7.00 (d, J = 16.4 Hz, 1H), 4.91–4.85 (m, 1H), 4.80–4.71 (m, 1H), 4.41 (dt, J = 26.9, 3.7 Hz, 2H), 3.27 (s, 3H), 1.46 (s, 9H). ^{13}C NMR (101 MHz, chloroform-d) δ 152.8, 144.4, 144.1, 133.0, 132.8, 132.6, 128.0, 127.3, 126.8, 126.7, 126.1, 125.6, 119.2, 113.2, 81.8 (d, J_{C-F} = 171 Hz), 69.4 (d, J_{C-F} = 21 Hz)., 37.3, 28.5. ^{19}F NMR (376 MHz, chloroform-d) δ −91.0 (m), −100.01(s).

tert-Butyl (E)-Ethyl(4-(3-(2-fluoroethoxy)-4-nitrostyryl)phenyl)-carbamate (27). The yellow sticky solid was purified on a silica flash column in 15% EtOAc:hexane, yield 0.110 g, (70%). ^{1}H NMR (400 MHz, chloroform-d) δ 7.91 (d, J = 8.4 Hz, 1H), 7.50 (d, J = 8.4 Hz, 2H), 7.24 (s, 1H), 7.24–7.21 (m, 2H), 7.21–7.19 (m, 1H), 7.18–7.16 (m, 2H), 7.02 (d, J = 16.3 Hz, 1H), 4.93–4.87 (m, 1H), 4.82–4.76 (m, 1H), 4.48–4.38 (m, 2H), 3.70 (q, J = 7.1 Hz, 2H), 1.46 (s, 9H), 1.17 (t, J = 7.1 Hz, 3H). ^{13}C NMR (101 MHz, chloroform-d) δ 152.7, 144.0, 143.1, 133.6, 132.5, 127.4, 127.1, 126.7, 126.2, 119.1, 113.2, 81.8 (d, J_{C-F} = 171 Hz), 69.4 (d, J_{C-F} = 21 Hz), 45.0, 28.5, 14.1. ^{19}F NMR (376 MHz, chloroform-d) δ −91.0 (m), −100.01(s).

tert-Butyl (E)-(4-(3-(2-Fluoroethoxy)-4-nitrostyryl)phenyl)-(propyl)carbamate (28). This yellow amorphous compound was purified on a silica flash column in 15% EtOAc:hexane, yield 0.150 g, (50%). ^{1}H NMR (400 MHz, chloroform-d) δ 7.89 (d, J = 8.5 Hz, 1H), 7.48 (d, J = 8.5 Hz, 2H), 7.22 (s, 1H), 7.21–7.18 (m, 2H), 7.16–7.13 (m, 2H), 7.00 (d, J = 16.3 Hz, 1H), 4.91–4.86 (m, 1H), 4.79–4.74 (m, 1H), 4.47–4.43 (m, 1H), 4.40–4.36 (m, 1H), 3.63–3.57 (m, 2H), 1.57 (d, J = 7.4 Hz, 1H), 1.53 (d, J = 5.8 Hz, 1H), 1.43 (s, 9H), 0.87 (t, J = 7.4 Hz, 3H). ^{13}C NMR (101 MHz, chloroform-d) δ 152.8, 144.0, 143.3, 133.6, 132.6, 127.4, 127.3, 126.7, 126.3, 119.2, 113.3, 81.8 (d, J_{C-F} = 171 Hz), 69.4 (d, J_{C-F} = 21 Hz), 51.7, 28.5, 22.0, 11.4. ^{19}F NMR (376 MHz, chloroform-d) δ −91.0 (m), −100.01(s).

tert-Butyl (E)-(4-(3-(2-Fluoroethoxy)-4-nitrostyryl)phenyl)-(isopropyl)carbamate (29). This yellow crystalline compound was purified on a silica flash column in 15% EtOAc:hexane, yield 0.165 g, (40.0%). ^{1}H NMR (400 MHz, chloroform-d) δ 7.91 (d, J = 8.4 Hz, 1H), 7.51 (d, J = 8.3 Hz, 2H), 7.24–7.20 (m, 1H), 7.19–7.17 (m, 2H), 7.14–7.09 (m, 2H), 7.05 (d, J = 16.3 Hz, 1H), 4.93–4.86 (m, 1H), 4.78 (d, J = 4.1 Hz, 1H), 4.57–4.49 (m, 1H), 4.48–4.37 (m, 2H), 1.39 (s, 9H), 1.13 (d, J = 6.8 Hz, 6H). ^{13}C NMR (101 MHz, chloroform-d) δ 152.8, 143.9, 134.8, 132.6, 130.5, 127.3, 126.7, 126.7, 119.2, 113.3, 81.8 (d, J_{C-F} = 171 Hz), 69.4 (d, J_{C-F} = 21 Hz), 48.9, 28.6, 21.8. ^{19}F NMR (376 MHz, chloroform-d) δ −91.0 (m), −100.01(s).

tert-Butyl (E)-sec-Butyl(4-(3-(2-fluoroethoxy)-4-nitrostyryl)-phenyl)carbamate (30). This yellow crystalline, compound was purified on a silica flash column in 15% EtOAc:hexane, yield 0.105 g (55%). ^{1}H NMR (500 MHz, chloroform-d) δ 7.96 (dd, J = 8.5, 1.9 Hz, 1H), 7.60–7.52 (m, 2H), 7.35–7.25 (m, 2H), 7.24 (s, 1H), 7.21–7.15

(m, 2H), 7.10 (dd, J = 16.3, 1.9 Hz, 1H), 4.89 (dt, J = 47.3, 3.0 Hz, 2H), 4.49 (dt, J = 26.9, 3.1 Hz, 2H), 4.28 (h, J = 7.3 Hz, 1H), 1.67 (dt, J = 9.9, 4.8 Hz, 2H), 1.46 (s, 9H), 1.18 (dd, J = 6.9, 1.9 Hz, 3H), 1.04 (td, J = 7.4, 1.8 Hz, 3H). ^{13}C NMR (126 MHz, chloroform-d) δ 155.1, 152.7, 143.9, 140.5, 138.9, 134.6, 132.5, 130.1, 127.2, 126.6, 126.6, 119.2, 113.3, 81.8 (d, J_{C-F} = 171 Hz), 69.4 (d, J_{C-F} = 21 Hz), 55.2, 28.7, 28.5, 19.6, 11.6. ^{19}F NMR (376 MHz, chloroform-d) δ −90.93 (tt, J = 47.3, 26.9 Hz), −100.01.

(E)-2-(2-Fluoroethoxy)-1-nitro-4-(4-nitrostyryl)benzene (31). The yellow amorphous, precipitate was washed with water and diethyl ether, yield 0.280 g, (80%). ^{1}H NMR (400 MHz, DMSO-d_6) δ 8.29 (d, J = 8.8 Hz, 2H), 7.96 (d, J = 8.5 Hz, 1H), 7.90 (d, J = 8.6 Hz, 2H), 7.66 (s, 2H), 7.59 (d, J = 16.4 Hz, 1H), 7.43 (d, J = 8.5 Hz, 1H), 4.80 (d, J = 47.4 Hz, 2H), 4.52 (d, J = 29.8 Hz, 2H). ^{13}C NMR (101 MHz, DMSO) δ 151.5, 143.1, 142.6, 131.2, 130.5, 127.8, 125.9, 124.2, 119.7, 113.2, 81.8 (d, J_{C-F} = 171 Hz), 69.4 (d, J_{C-F} = 21 Hz). ^{19}F NMR (376 MHz, DMSO) δ −89.76, −89.84.

General Method for the Boc-Deprotection and Reduction (32–39, Scheme 5, Step (ii)). To a 100 mL round-bottom flask fitted with a stirring bar was added tin(II) chloride (10 equiv). The compound to be reduced (**26–31, 38**) was dissolved in ethyl acetate (25 mL) and ethanol (15 mL) and added to tin(II) chloride. The mixture was fitted with a water condenser, heated to 80 °C for 6 h open to air in the dark. The reaction were monitored through TLC, and after completion, solvent was removed by vacuum. The residue was quenched by aq Na$_2$CO$_3$ (20%) until bubbles stopped forming. The compound was extracted in ethyl acetate (30 mL × 3) three times and washed with aq Na$_2$CO$_3$ (20%) 2 times (30 mL × 2) and once with water (50 mL) followed by brine (50 mL). It was then dried over Na$_2$SO$_4$, and solvent was removed by reducing the pressure. The crude product was dissolved in a minimal DCM slurry on silica and purified on silica by flash column chromatography using 10−15% EtOAc:hexane.[30]

(E)-4-(4-Amino-3-(2-fluoroethoxy)styryl)-N-methylaniline (32). The brown amorphous compound was purified on a silica flash column and eluted with 20% EtOAc:hexane, yield 0.02 g, (55%). ^{1}H NMR (400 MHz, chloroform-d) δ 7.38 (d, J = 8.6 Hz, 2H), 7.00 (dd, J = 4.2, 2.4 Hz, 2H), 6.87 (d, J = 1.9 Hz, 2H), 6.75 (d, J = 8.4 Hz, 1H), 6.68–6.60 (m, 2H), 4.93–4.75 (m, 2H), 4.40–4.29 (m, 2H), 2.91 (s, 3H). ^{13}C NMR (101 MHz, chloroform-d) δ 148.9, 146.3, 129.4, 127.6, 127.5, 125.9, 125.0, 120.9, 115.6, 112.8, 112.8, 112.7, 112.7, 110.0, 81.2 (d, J_{C-F} = 181 Hz), 68.1 (d, J_{C-F} = 21 Hz), 30.9. ^{19}F NMR (376 MHz, chloroform-d) δ −90.53 − −91.75 (m), −100.01. HR-MS (ESI) m/z calculated for (C$_{17}$H$_{19}$FN$_2$O) [M + H]$^+$ 287.1554, found 287.1550. HPLC purity: 96.26%, retention time 10.07 min.

(E)-4-(4-Amino-3-(2-fluoroethoxy)styryl)-N-ethylaniline (33). The brown amorphous compound was purified on a silica flash column and eluted with 20% EtOAc:hexane, yield 0.045 g (64%). ^{1}H NMR (400 MHz, chloroform-d) δ 7.34–7.29 (m, 2H), 6.97–6.93 (m, 2H), 6.81 (d, J = 1.6 Hz, 2H), 6.70 (d, J = 8.4 Hz, 1H), 6.63–6.56 (m, 2H), 4.91–4.70 (m, 2H), 4.38–4.24 (m, 2H), 3.88 (s, 2H), 3.18 (q, J = 7.2 Hz, 2H), 1.26 (t, J = 7.1 Hz, 3H). ^{13}C NMR (101 MHz, chloroform-d) δ 146.6, 145.8, 135.7, 128.9, 127.1, 126.7, 125.4, 124.3, 120.4, 115.1, 113.1, 109.5, 81.8 (d, J_{C-F} = 171 Hz), 67.7 (d, J_{C-F} = 20 Hz), 38.3, 14.7. ^{19}F NMR (376 MHz, chloroform-d) δ −91.36 (tt, J = 47.6, 28.1 Hz), −100.01. HR-MS (ESI) m/z calculated for (C$_{18}$H$_{21}$FN$_2$O) [M + H]$^+$ 301.1711, found 301.1706. HPLC purity: 100.0%, retention time 13.12 min. C-18 reversed-phase HPLC (Phenomenex, 10 × 250 mm), eluent: acetonitrile:H$_2$O = 60:40, flow rate of 3.0 mL/min.

(E)-4-(4-Amino-3-(2-fluoroethoxy)styryl)-N-propylaniline (34). The brown amorphous compound was purified on a silica flash column and eluted with 20% EtOAc:hexane, yield 0.070 g, (70%). ^{1}H NMR (400 MHz, chloroform-d) δ 7.31 (d, J = 8.6 Hz, 2H), 6.95 (dt, J = 4.2, 2.2 Hz, 2H), 6.81 (d, J = 2.0 Hz, 2H), 6.70 (d, J = 8.4 Hz, 1H), 6.58 (d, J = 8.6 Hz, 2H), 4.90–4.80 (m, 1H), 4.77–4.69 (m, 1H), 4.38–4.25 (m, 2H), 3.84 (s, 3H), 3.11 (t, J = 7.1 Hz, 2H), 1.65 (h, J = 7.3 Hz, 2H), 1.01 (t, J = 7.4 Hz, 3H). ^{13}C NMR (101 MHz, chloroform-d) δ 147.9, 146.1, 136.0, 129.2, 127.4, 127.1, 125.7, 124.7, 120.7, 115.4, 112.9, 109.8, 82.1 (d, J_{C-F} = 171 Hz, 1C), 68.0 (d, J_{C-F} = 20 Hz, 1C), 45.9, 22.8, 11.8. ^{19}F NMR (376 MHz, chloroform-d) δ

−91.36 (tt, J = 47.7, 28.2 Hz), −100.01. HR-MS (ESI) m/z calculated for ($C_{19}H_{23}FN_2O$) [M + H]$^+$ 315.1867, found 315.1866. HPLC purity: 100.0%, retention time 17.37 min. C-18 reversed-phase HPLC (Phenomenex, 10 × 250 mm), eluent: acetonitrile:H_2O = 60:40, flow rate of 3.0 mL/min.

(E)-4-(4-Amino-3-(2-fluoroethoxy)styryl)-N-isopropylaniline **(35)**. The yellow amorphous compound was purified on a silica flash column and eluted with 20% EtOAc:hexane, yield 0.10 g (90%). ^{1}H NMR (400 MHz, chloroform-d) δ 7.30 (d, J = 8.7 Hz, 2H), 6.95 (dq, J = 4.3, 1.8 Hz, 2H), 6.81 (d, J = 1.8 Hz, 2H), 6.69 (d, J = 8.4 Hz, 1H), 6.56 (d, J = 8.6 Hz, 2H), 4.89−4.81 (m, 1H), 4.77−4.72 (m, 1H), 4.41−4.26 (m, 2H), 3.87 (s, 2H), 3.65 (p, J = 6.3 Hz, 1H), 1.22 (d, J = 6.3 Hz, 6H). ^{13}C NMR (101 MHz, chloroform-d) δ 146.6, 145.8, 135.7, 128.9, 127.1, 126.7, 125.4, 124.3, 120.4, 115.1, 113.1, 109.5, 81.8 (d, J_{C-F} = 171 Hz,), 67.7 (d, J_{C-F} = 20 Hz,), 44.0, 22.8. ^{19}F NMR (376 MHz, chloroform-d) δ −91.36 (tt, J = 47.6, 28.1 Hz), −100.01. HR-MS (ESI) m/z calculated for ($C_{19}H_{23}FN_2O$) [M + H]$^+$ 315.1867, found 315.1867. HPLC purity: 100.0%, retention time 16.22 min. C-18 reversed-phase HPLC (Phenomenex, 10 × 250 mm), eluent: acetonitrile:H_2O = 60:40, flow rate of 3.0 mL/min.

(E)-4-(4-Amino-3-(2-fluoroethoxy)styryl)-N-(sec-butyl)aniline **(36)**. This brown amorphous compound was purified on a silica flash column and eluted with 20% EtOAc:hexane, yield 0.040 g (70%). ^{1}H NMR (400 MHz, chloroform-d) δ 7.33−7.27 (m, 2H), 6.95 (dt, J = 4.4, 2.0 Hz, 2H), 6.80 (d, J = 2.5 Hz, 2H), 6.69 (d, J = 8.4 Hz, 1H), 6.58−6.53 (m, 2H), 4.88−4.83 (m, 1H), 4.77−4.70 (m, 1H), 4.36−4.32 (m, 1H), 4.30−4.24 (m, 1H), 3.82 (s, 3H), 3.42 (q, J = 6.3 Hz, 1H), 1.69−1.57 (m, 1H), 1.53−1.44 (m, 1H), 1.18 (d, J = 6.3 Hz, 3H), 0.97 (d, J = 7.4 Hz, 3H). ^{13}C NMR (101 MHz, chloroform-d) δ 147.1, 146.1, 136.0, 129.3, 127.5, 126.9, 125.8, 124.6, 120.7, 115.4, 113.3, 109.9, 82.1 (d, J_{C-F} = 171 Hz), 68.1 (d, J_{C-F} = 20 Hz), 50.0, 29.8, 20.4, 10.5. ^{19}F NMR (376 MHz, chloroform-d) δ −91.39 (tt, J = 47.5, 27.9 Hz), −100.01. HR-MS (ESI) m/z calculated for ($C_{20}H_{25}FN_2O$) [M + H]$^+$ 329.2024, found 329.2020. HPLC purity: 100.0%, retention time 23.37 min. C-18 reversed-phase HPLC (Phenomenex, 10 × 250 mm), eluent: acetonitrile:H_2O = 60:40, flow rate of 3.0 mL/min.

(E)-4-(4-Aminostyryl)-2-(2-fluoroethoxy)aniline **(37)**. This dark red amorphous compound was purified on a silica flash column and eluted with 20% EtOAc:hexane, yield 0.085 g (64%). ^{1}H NMR (400 MHz, chloroform-d) δ 7.31 (d, J = 8.5 Hz, 2H), 6.97 (dq, J = 3.2, 1.8 Hz, 2H), 6.84 (s, 2H), 6.71 (d, J = 8.5 Hz, 1H), 6.70−6.66 (m, 2H), 4.90−4.71 (m, 2H), 4.38−4.25 (m, 2H), 3.82 (s, 4H). ^{13}C NMR (101 MHz, chloroform-d) δ 146.2, 145.8, 136.3, 129.0, 128.7, 127.5, 125.6, 120.9, 115.5, 109.9, 82.2 (d, J_{C-F} = 171 Hz), 68.1 (d, J_{C-F} = 20 Hz). ^{19}F NMR (376 MHz, chloroform-d) δ −90.99 − −91.82 (m), −100.01. HR-MS (ESI) m/z calculated for ($C_{16}H_{17}FN_2O$) [M + H]$^+$ 273.1398, found 273.1396. HPLC purity: 100.0%, retention time 7.07 min. C-18 reversed-phase HPLC (Phenomenex, 10 × 250 mm), eluent: acetonitrile:H_2O = 60:40, flow rate of 3.0 mL/min.

tert-Butyl (E)-(4-(4-(2-Fluoroethoxy)-3-nitrostyryl)phenyl)-(methyl)carbamate **(38)**. Following the general method of Wittig−Horner reaction as described above, compound **38** was synthesized as a yellow sticky solid, which was purified on silica flash column in 15% EtOAc:hexane, yield 0.265 g (75%). ^{1}H NMR (400 MHz, chloroform-d) δ 7.92 (d, J = 2.2 Hz, 1H), 7.58 (dd, J = 8.7, 2.3 Hz, 1H), 7.42−7.38 (m, 2H), 7.24−7.18 (m, 2H), 7.04 (d, J = 8.7 Hz, 1H), 6.94 (d, J = 12.2 Hz, 2H), 4.83−4.77 (m, 1H), 4.74−4.67 (m, 1H), 4.40−4.28 (m, 2H), 3.24 (s, 3H), 1.43 (s, 9H). ^{13}C NMR (101 MHz, chloroform-d) δ 154.3, 150.6, 143.4, 133.2, 131.4, 131.3, 131.0, 129.1, 128.9, 127.0, 126.4, 125.2, 125.0, 122.78, 115.3, 81.2 (d, J_{C-F} = 181 Hz), 69.0 (d, J_{C-F} = 21 Hz), 36.9, 28.1. ^{19}F NMR (376 MHz, chloroform-d) δ −90.96 (tt, J = 47.3, 27.1 Hz), −100.01.

(E)-4-(4-(2-Fluoroethoxy)-3-nitrostyryl)-N-methylaniline **(39)**. Following the general method of [Boc-deprotection and reduction](#) as described above, compound **39** was synthesized as an off-white amorphous compound, which was purified through precipitation out of EtOAc:hexane (2:3), yield 0.050 g (30%). ^{1}H NMR (500 MHz, chloroform-d) δ 7.33 (d, J = 8.0 Hz, 2H), 6.90 (s, 1H), 6.85 (s, 1H), 6.80 (s, 1H), 6.76 (s, 1H), 6.67 (s, 1H), 6.59 (d, J = 8.1 Hz, 2H), 4.81

(s, 1H), 4.72 (s, 1H), 4.25 (d, J = 27.1 Hz, 2H), 3.84 (s, 4H), 2.86 (s, 3H). ^{13}C NMR (126 MHz, DMSO) δ 149.3, 144.5, 138.0, 131.4, 127.2, 126.3, 125.0, 123.4, 114.9, 112.5, 111.7, 110.9, 82.4 (d, J_{C-F} = 166 Hz), 67.8 (d, J_{C-F} = 19 Hz). 29.6. ^{19}F NMR (376 MHz, chloroform-d) δ −90.96 (tt, J = 47.3, 27.1 Hz), −100.01. HR-MS (ESI) m/z calculated for ($C_{17}H_{19}FN_2O$) [M + H]$^+$ 287.1554, found 287.1552. HPLC purity: >99%, retention time 10.25 min. C-18 reversed-phase HPLC (Phenomenex, 10 × 250 mm), eluent: acetonitrile:H_2O = 60:40, flow rate of 3.0 mL/min.

Animal Preparation and Studies. All animal experiments were performed in accordance with guidance protocol approved by the Institutional Animal Care and Use Committee (IACUC) of Case Western Reserve University (Protocol 2013-0016, 2013-0017). The animals were subjected to minimal stress during tail vein injections. The 8 week old wild-type C57BL/6 mice (Jackson Laboratory, Bar Harbor, MN) were used for all of the in vitro and ex vivo tissue staining, and SD rats (Harlan Laboratory, Indianaplis, IN) were used for microPET/CT imaging studies. The rats were fasted overnight prior to imaging, but had access to water. Their diet was then replenished after microPET/CT imaging.

In Vitro Tissue Staining and Assay of Fluorecent Intensity. Wild-type mice (20−22g, 8 weeks old) were deeply anesthetized and perfused transcardially with precooled saline (4 °C, 10 mL/min for 1 min followed by 7 mL/min for 6 min) followed by fixation with precooled 4% PFA in PBS (4 °C, 10 mL/min for 1 min followed by 7 mL/min for 6 min). Brain tissues were then removed, postfixed by immersion in 4% PFA overnight, dehydrated in 10%, 20%, and 30% sucrose solution, embedded in a freezing compound (OCT, Fisher Scientific, Suwanee, GA), and sectioned at 20 μm with a cryostat (Thermo HM525, Thermo Fisher Scientific Inc., Chicago, IL, USA). Brain sections were collected from AP (1.0) to AP (−0.1)^{33} and in 12 sections were mounted in order on the bottom of 12 superfrost slides (Fisher Scientific) with one section on each slide. Sections 13−24 were mounted in order on the middle of each slide, and sections 25−36 were mounted in order on the top of each slide. Sections were then incubated with tested compounds (1 mM, 5% DMSO in 1 × PBS (pH 7.0), 6 sections per compound) for 25 min at room temperature in the dark. Excess compounds were washed by briefly rinsing the slides in PBS (1×) and coverslipped with fluoromount-G mounting media (Vector Laboratories, Burlingame, CA). Sections were then examined under a microscope (Leica DM4000B, Leica Microsystem Inc., Buffalo Grove, IL, USA) equipped for fluorescence (DFC7000T), and images of the stained mouse whole brain sections were acquired with the same exposure time.

ImageJ software was then used to quantify pixel intensity values on 6 sections of each tested compound. A ROI was selected on the genu of the corpus callosum (gcc, white matter), and the same size ROI was applied on the midline between gcc and the edge of the section (see Figure 2A), which is considered as gray matter. Images were analyzed by two experienced individuals. The FIR of white matter to gray matter were then calculated.

Ex Vivo Imaging. Wild-type mice were administered with the newly synthesized compounds (40 mg/kg) via tail vein injection, and 30 min later, the mice were perfused transcardially with saline followed by 4% PFA in PBS. Brain tissues were then removed, postfixed by immersion in 4% PFA overnight, dehydrated in 30% sucrose solution, cryostat sectioned at 100 μm, and mounted on superfrost slides, and images were acquired directly using a Leica fluorescent microscope.

Radiosynthesis. No carrier-added (n.c.a.) [^{18}F] fluoride was produced by a cyclotron (Eclipse High Production, Siemens) via the nuclear reaction ^{18}O (p,n) ^{18}F. At the EOB, the activity of aqueous [^{18}F] fluoride (50−100 mCi) was transferred to the GE Tracerlab FXn synthesizer with high helium pressure.

After delivery, the radioactive solution was passed through a Sep-Pak light QMA cartridge (Waters, WAT023525, 130 mg, 37−55 μm, preconditioned with 5 mL of water followed by 10 mL of air in syringe) and was eluted with K_2CO_3 solution (6 mg, 0.043 mmol, in 0.6 mL water) followed by K_{222} solution (12 mg, 0.032 mmol, in 1 mL acetonitrile). The solvent was evaporated under a steam of helium at 85 °C for 5 min, and the residue was vacuumed at 55 °C for another 3

min to get the anhydrous $K_{222}/[^{18}F]$ complex. A solution of the tosylated precursors (3−5 mg, 0.0062−0.011 mmol, in 0.8 mL acetonitrile) was added to the above dried complex, and the mixture was heated at 110 °C for 10 min. Ethyl acetate (3 mL) and hexane (2 mL) were added to the reaction vessel, and the mixture was passed through a preconditioned Sep-Pak silica cartridge (Waters, WAT 020520, 690 mg, 55−105 μm, preconditioned with 5 mL of ether). The solvent was removed under a steam of helium at 70 °C, and the residue was added to a tin chloride solution (30 mg, 0.16 mmol, in 1 mL ethanol and 0.5 mL HCl (1 M). The resulting mixture was heated at 115 °C for 10−20 min. A NaOH solution (0.8 mL, 1 M) and water (15 mL) were then added, and the resulting mixture was passed through a preconditioned Sep-Pak C-18 cartridge (Waters, WAT020515, 360 mg, 55−105 μm, preconditioned with 5 mL of ethanol followed by 10 mL of water, then dried by 10 mL of air in a syringe). The cartridge was washed with another 20 mL of water, and the crude products were eluted with 1 mL acetonitrile which was further purified by semipreparative HPLC (Phenomenex C-18, 10 × 250 mm, acetonitrile:H_2O = 60:40, flow rate of 5 mL/min, t_R = 6−14 min). The radioactive fraction containing the desired products was collected, diluted with water, loaded onto a Sep-Pak C-18 cartridge, and eluted with 1 mL ethanol. After evaporation, the residue was redissolved in 5% ethanol in saline solution and filtered (0.22 μm) into a sterile injection bottle for animal use. RCP and specific activity (SA) were determined by analytical HPLC (Phenomenex C-18, 4.6 × 250 mm, acetonitrile:H_2O = 65:35, flow rate of 1 mL/min, t_R = 6−10 min). SA was calculated by area of the UV peak of purified F-18 compound and titrated with the standard curve of the nonradioactive reference compound of known concentration.

MicroPET/CT Image Acquisition and Analysis. MicroPET/CT imaging was performed using a Siemens Inveon microPET/CT scanner in the Case Center for Imaging Research. For better anatomic localization, CT coregistration was applied. Before microPET imaging, CT scout views were taken to ensure the brain tissues were placed in the coscan field of view (FOV) where the highest image resolution and sensitivity are achieved. Under anesthesia, radiotracers (1−2 mCi) were administered via tail vein injection and immediately followed by a dynamic PET acquisition up to 60 min. Once microPET acquisition was done, the rat was moved into the CT field and a two-bed CT scan was performed. A two-dimensional ordered subset expectation maximization (OSEM) algorithm was used for image reconstruction using CT for the attenuation correction. For quantitative analysis, the resultant PET images were registered to the CT images which enabled us to accurately define the ROI and quantify the radioactivity concentrations. In this study, the whole brain of rat was used as ROI, and the radioactivity concentrations were determined in terms of SUV.

In Situ Autoradiography. *Ex vivo.* Wild-type mice were euthanized at 10 min post i.v. injection of $[^{18}F]$**32** (3.0 mCi). The brains were rapidly removed, placed in optimal cutting temperature (OCT) embedding medium and frozen at −20 °C. After reaching equilibrium at this temperature, the brains were coronally cryostat sectioned at 60 μm on a cryostat and mounted on superfrost slides. After drying by air at room temperature, the slides were put in a cassette and exposed to film to obtain images.

Ex vivo block. For ex vivo blocking studies, mice were pretreated with CIC, a compound which has proved to bind to myelin with high affinity and specificity (i.v. 160 mg/kg) 3 h before injection of $[^{18}F]$**32** (3.0 mCi). Mice were then euthanized, and brains were removed and sectioned. After drying by air, the slides were put in a cassette and exposed to film to obtain images.

Biostability of $[^{18}F]$32 in Wild-Type Mice. The in vivo biostability of $[^{18}F]$**32** in plasma was analyzed using radio-HPLC. Briefly, mice ($n = 3$) were sacrificed at 5, 30, and 60 min postinjection of $[^{18}F]$**32** (0.8−1.0 mCi) through tail vein. Blood was collected into VACUETTE blood collection tubes which were precoated with K3EDTA (containing 4.0 mg of K3EDTA, Greiner Bio One, Germany). The samples were centrifuged at 3000 rpm for 5 min at 4 °C to separate plasma. The supernatant plasma samples were mixed with ice-cold methanol and centrifuged again at 10,000 rpm for 3 min to further remove proteins and other biological matrix. The

supernatant was then analyzed by radio-HPLC using acetonitrile/water (60:40, v/v) as mobile phase at a flow rate of 1.0 mL/min. The percentage of parent compound was then calculated.

ASSOCIATED CONTENT

$\textcircled{S}$ Supporting Information

The Supporting Information is available free of charge on the ACS Publications website at DOI: 10.1021/acs.jmedchem.5b01858.

> Additional figures, NMR spectra, HPLC spectra, HRMS spectra (PDF)
> 3D movie of imaging (AVI)
> Compound data (CSV)

AUTHOR INFORMATION

Corresponding Author

*E-mail: yxw91@case.edu. Phone: 216-844-3288. Fax: 216-844-8062.

Present Addresses

^{O}Beachwood High School, Beachwood, OH 44122, United States.

$^\nabla$Phillips Academy, Andover, MA 01810, United States.

Author Contributions

#These authors contributed equally.

Notes

The authors declare no competing financial interest.

ABBREVIATIONS USED

s, singlet; br s, broad singlet; dd, doublet of doublets; ddd, doublet of doublet of doublets; br d, broad doublets; t, triplet; dt, triplets of doublets; q, quartet; m, multiplet; br m, broad multiplet; MTR, magnetization transfer ratio; MeDAS, methyl diamino stilbene; K_{222}, 4,7,13,16,21,24-hexaoxa-1,10-diazabicyclo[8.8.8]hexacosane; NaH, sodium hydride; $SnCl_2$, stannous chloride; K_2CO_3, potassium carbonate; EtOAc, ethyl acetate; MeCN, acetonitrile; EtOH, ethanol; SUV, standardized uptake value; ROI, region of interest; CT, computerized tomography; d, deuterated; PFA, paraformaldehyde; FOV, field of view; OSEM, ordered subset expectation maximization; RPC, radiochemical purity; SA, specific activity

REFERENCES

(1) Quarles, R. H.; Macklin, W. M; Morella, P. Myelin Formation, Structure, and Biochemistry. In *Basic Neurochemistry, Molecular, Cellular and Medical Aspects*, 7th ed.; Siegel, G. J, Albers, R. W., Brady, S. T., Price, D. L., Eds.; Elsevier Academic: Burlington, MA, 2006; pp 51−72.

(2) Nave, K. A. Myelination and Support of Axonal Integrity by Glia. *Nature* **2010**, *468*, 244−252.

(3) Trapp, B. D.; Nave, K. A. Multiple Sclerosis: an Immune or Neurodegenerative Disorder? *Annu. Rev. Neurosci.* **2008**, *31*, 247−269.

(4) Polman, C. H.; Reingold, S. C.; Edan, G.; Filippi, M.; Hartung, H. P.; Kappos, L.; Lublin, F. D.; Metz, L. M.; McFarland, H. F.; O'Connor, P. W.; Sandberg-Wollheim, M.; Thompson, A. J.; Weinshenker, B. G.; Wolinsky, J. S. Diagnostic Criteria for Multiple

Sclerosis: 2005 Revisions to the "McDonald Criteria". *Ann. Neurol.* **2005**, *58*, 840−846.

(5) Filippi, M.; Falini, A.; Arnold, D. L.; Fazekas, F.; Gonen, O.; Simon, J. H.; Dousset, V.; Savoiardo, M.; Wolinsky, J. S. Magnetic Resonance Techniques for the in Vivo Assessment of Multiple sclerosis Pathology: Consensus Report of the White Matter Study Group. *J. Magn. Reson. Imaging* **2005**, *21*, 669−675.

(6) Molyneux, P. D.; Barker, G. J.; Barkhof, F.; Beckmann, K.; Dahlke, F.; Filippi, M.; Ghazi, M.; Hahn, D.; MacManus, D.; Polman, C.; Pozzilli, C.; Kappos, L.; Thompson, A. J.; Wagner, K.; Yousry, T.; Miller, D. H. European Study Group on Interferon Beta-1b in Secondary Progressive, M. S. Clinical-MRI Correlations in a European Trial of Interferon beta-1b in Secondary Progressive MS. *Neurology* **2001**, *57*, 2191−2197.

(7) McFarland, H. F.; Frank, J. A.; Albert, P. S.; Smith, M. E.; Martin, R.; Harris, J. O.; Patronas, N.; Maloni, H.; McFarlin, D. E. Using Gadolinium-Enhanced Magnetic Resonance Imaging Lesions to Monitor Disease Activity in Multiple Sclerosis. *Ann. Neurol.* **1992**, *32*, 758−766.

(8) Le Bihan, D.; Mangin, J. F.; Poupon, C.; Clark, C. A.; Pappata, S.; Molko, N.; Chabriat, H. Diffusion Tensor Imaging: Concepts and Applications. *J. Magn. Reson. Imaging* **2001**, *13*, 534−546.

(9) Harris, G. J.; Rhew, E. H.; Noga, T.; Pearlson, G. D. User-Friendly Method for Rapid Brain and CSF Volume Calculation Using Transaxial MRI Images. *Psychiatry Res., Neuroimaging* **1991**, *40*, 61−68.

(10) Phelps, M. E. Positron Emission Tomography Provides Molecular Imaging of Biological Processes. *Proc. Natl. Acad. Sci. U. S. A.* **2000**, *97*, 9226−9233.

(11) Wilms, H.; Claasen, J.; Rohl, C.; Sievers, J.; Deuschl, G.; Lucius, R. Involvement of Benzodiazepine Receptors in Neuroinflammatory and Neurodegenerative Diseases: Evidence from Activated Microglial Cells in-vitro. *Neurobiol. Dis.* **2003**, *14*, 417−424.

(12) Cuzner, M. L. Microglia in Health and Disease. *Biochem. Soc. Trans.* **1997**, *25*, 671−673.

(13) Chen, M. K.; Guilarte, T. R. Imaging the Peripheral Benzodiazepine Receptor Response in Central Nervous System Demyelination and Remyelination. *Toxicol. Sci.* **2006**, *91*, 532−539.

(14) Wu, C.; Tian, D.; Feng, Y.; Polak, P.; Wei, J.; Sharp, A.; Stankoff, B.; Lubetzki, C.; Zalc, B.; Mufson, E. J.; Gould, R. M.; Feinstein, D. L.; Wang, Y. A Novel fluorescent Probe That Is Brain Permeable and Selectively Binds to Myelin. *J. Histochem. Cytochem.* **2006**, *54*, 997−1004.

(15) Wu, C.; Wei, J.; Tian, D.; Feng, Y.; Miller, R. H.; Wang, Y. Molecular Probes for Imaging Myelinated White Matter in CNS. *J. Med. Chem.* **2008**, *51*, 6682−6688.

(16) Wang, C.; Popescu, D. C.; Wu, C.; Zhu, J.; Macklin, W.; Wang, Y. In Situ Fluorescence Imaging of Myelination. *J. Histochem. Cytochem.* **2010**, *58*, 611−621.

(17) Stankoff, B.; Wang, Y.; Bottlaender, M.; Aigrot, M. S.; Dolle, F.; Wu, C.; Feinstein, D.; Huang, G. F.; Semah, F.; Mathis, C. A.; Klunk, W.; Gould, R. M.; Lubetzki, C.; Zalc, B. Imaging of CNS Myelin by Positron-Emission Tomography. *Proc. Natl. Acad. Sci. U. S. A.* **2006**, *103*, 9304−9309.

(18) Wang, Y.; Wu, C.; Caprariello, A. V.; Somoza, E.; Zhu, W.; Wang, C.; Miller, R. H. In vivo Quantification of Myelin Changes in the Vertebrate Nervous System. *J. Neurosci.* **2009**, *29*, 14663−14669.

(19) Wu, C.; Zhu, J.; Baeslack, J.; Zaremba, A.; Hecker, J.; Kraso, J.; Matthews, P. M.; Miller, R. H.; Wang, Y. Longitudinal Positron Emission Tomography Imaging for Monitoring Myelin Repair in the Spinal cord. *Ann. Neurol.* **2013**, *74*, 688−698.

(20) de Paula Faria, D.; de Vries, E. F.; Sijbesma, J. W.; Buchpiguel, C. A.; Dierckx, R. A.; Copray, S. C. PET Imaging of Glucose Metabolism, Neuroinflammation and Demyelination in the Lysoleci-thin Rat Model for Multiple Sclerosis. *Mult. Scler.* **2014**, *20*, 1443−1452.

(21) de Paula Faria, D.; Copray, S.; Sijbesma, J. W.; Willemsen, A. T.; Buchpiguel, C. A.; Dierckx, R. A.; de Vries, E. F. PET Imaging of Focal Demyelination and Remyelination in a Rat Model of Multiple Sclerosis: Comparison of [11C]MeDAS, [11C]CIC and [11C]PIB. *Eur. J. Nucl. Med. Mol. Imaging* **2014**, *41*, 995−1003.

(22) de Paula Faria, D.; de Vries, E. F.; Sijbesma, J. W.; Dierckx, R. A.; Buchpiguel, C. A.; Copray, S. PET Imaging of Demyelination and Remyelination in the Cuprizone Mouse Model for Multiple Sclerosis: a Comparison Between [11C]CIC and [11C]MeDAS. *NeuroImage* **2014**, *87*, 395−402.

(23) Ryzhikov, N. N.; Seneca, N.; Krasikova, R. N.; Gomzina, N. A.; Shchukin, E.; Fedorova, O. S.; Vassiliev, D. A.; Gulyas, B.; Hall, H.; Savic, I.; Halldin, C. Preparation of Highly Specific Radioactivity [18F]flumazenil and Its Evaluation in Cynomolgus Monkey by Positron Emission Tomography. *Nucl. Med. Biol.* **2005**, *32*, 109−116.

(24) Chaly, T.; Dhawan, V.; Kazumata, K.; Antonini, A.; Margouleff, C.; Dahl, J. R.; Belakhlef, A.; Margouleff, D.; Yee, A.; Wang, S.; Tamagnan, G.; Neumeyer, J. L.; Eidelberg, D. Radiosynthesis of [18F] N-3-Fluoropropyl-2-Beta-Carbomethoxy-3-Beta-(4-Iodophenyl) Nor-tropane and the First Human Study with Positron Emission Tomography. *Nucl. Med. Biol.* **1996**, *23*, 999−1004.

(25) Park, C.; Lee, B. S.; Chi, D. Y. High Efficiency Synthesis of F-18 Fluoromethyl Ethers: an Attractive Alternative for C-11 Methyl Groups in Positron Emission Tomography Radiopharmaceuticals. *Org. Lett.* **2013**, *15*, 4346−4349.

(26) Shao, X.; Hockley, B. G.; Hoareau, R.; Schnau, P. L.; Scott, P. J. Fully Automated Preparation of [11C]Choline and [18F]-Fluoromethylcholine Using TracerLab Synthesis Modules and Facilitated Quality Control Using Analytical HPLC. *Appl. Radiat. Isot.* **2011**, *69*, 403−409.

(27) Wang, C.; Wu, C.; Zhu, J.; Miller, R. H.; Wang, Y. Design, Synthesis, and Evaluation of Coumarin-Based Molecular Probes for Imaging of Myelination. *J. Med. Chem.* **2011**, *54*, 2331−2340.

(28) Frullano, L.; Zhu, J.; Miller, R. H.; Wang, Y. Synthesis and Characterization of a Novel Gadolinium-Based Contrast Agent for Magnetic Resonance Imaging of Myelination. *J. Med. Chem.* **2013**, *56*, 1629−1640.

(29) Yousefi, B. H.; Drzezga, A.; von Reutern, B.; Manook, A.; Schwaiger, M.; Wester, H. J.; Henriksen, G. A Novel ^{18}F-labeled Imidazo[2,1-b]Benzothiazole (IBT) for High-Contrast PET Imaging of Beta-Amyloid Plaques. *ACS Med. Chem. Lett.* **2011**, *2*, 673−677.

(30) Condie, A. G.; Gerson, S. L.; Miller, R. H.; Wang, Y. Two-Photon Fluorescent Imaging of Myelination in the Spinal Cord. *ChemMedChem* **2012**, *7*, 2194−2203.

(31) Parhi, A. K.; Wang, J. L.; Oya, S.; Choi, S. R.; Kung, M. P.; Kung, H. F. 2-(2′-((Dimethylamino)Methyl)-4′-(Fluoroalkoxy)-Phenylthio)Benzenamine Derivatives as Serotonin Transporter Imaging Agents. *J. Med. Chem.* **2007**, *50*, 6673−6684.

(32) Snellman, A.; Rokka, J.; Lopez-Picon, F. R.; Eskola, O.; Wilson, I.; Farrar, G.; Scheinin, M.; Solin, O.; Rinne, J. O.; Haaparanta-Solin, M. Pharmacokinetics of [18]Flutemetamol in Wild-Type Redents and Its Binding to Beta Amyloid Deposits in a Mouse Model of Alzheimer's Disease. *Eur. J. Nucl. Med. Mol. Imaging* **2012**, *39*, 1784−1795.

(33) George, P.; Watson, C. *The Rat Brain in Stereotaxic Coordinates*, 6th ed. Elsevier Inc.: London, UK, 2007; pp 68−85.